Department of Chemistry
University of Oslo

Development and Application of Relativistic Quantum Chemical Methods

Jon K. Lærdahl

Dissertation for the degree of Doctor Scientiarum

Oslo, 1997

Contents

List of papers

This thesis is based on the following publications and manuscripts.

I. J.K. Laerdahl, T. Saue, K. Fægri jr. and H.M. Quiney, *Ab initio study of PT-odd interactions in thallium fluoride*, Phys. Rev. Lett. **79**, 1642 (1997).

II. H.M. Quiney, J.K. Laerdahl, K. Fægri jr. and T. Saue, *Ab initio Dirac-Hartree-Fock calculations of chemical properties and PT-odd effects in thallium fluoride*, Phys. Rev. A (accepted for publication).

III. J.K. Laerdahl, T. Saue and K. Fægri jr., *Direct relativistic MP2: properties of ground state CuF, AgF and AuF*, Theor. Chem. Acc. **97**, 177 (1997).

IV. J.K. Laerdahl, K. Fægri jr., L. Visscher and T. Saue, *A fully relativistic Dirac–Hartree–Fock and MP2 study of the lanthanide and actinide contraction*, (manuscript).

Chapter 1

Introduction

Quantum chemistry is the study of spectroscopic constants, chemical processes, interactions, reactions and all the other things we wish to know about molecules studied by methods of quantum mechanics. Since they were introduced in the first half of this century, the quantum chemical models have had a large conceptual impact on chemistry. Researchers in many areas of chemistry use terms adopted from quantum chemistry such as molecular orbitals, energy levels, hybridization and resonance theory, and use quantum chemical models to explain their observations. At the same time the development of efficient algorithms and the enormous increase in computational resources due to the development of modern computers have actually made it possible to perform *ab initio* calculations, that is, calculations from first principles, of chemical properties. Qualitative calculations can be made for small to medium sized molecules (less than ten atoms), and often with precision that competes with the experimental results that are obtained in the laboratory.

The development of the theoretical structure we call quantum mechanics between 1925 and 1928 and the immediate success of the theory in explaining many atomic and chemical problems lead Dirac in 1929 to remark that 'The underlying physical laws necessary for the mathematical theory of a large part of physics and the whole of chemistry are thus completely known' [1]. Since then quantum chemical methods based on the Schrödinger equation have been employed with considerable success. Even if it is not possible to solve the equations analytically for systems more complicated than the hydrogen atom excellent approximate solutions may be found. In practice it is only the computational resources that limits the accuracy, and therefore the development of modern computers has been of great importance.

In molecular calculations one usually employs the quantum chemical basis for the molecular 'ball–and–stick' model, the Born–Oppenheimer approximation, and assumes that the motion of the electrons and atomic nuclei can be separated. Most theoretical work then starts off with the independent-particle model or Hartree–Fock model, where each

electron is treated as moving in the average field of the other electrons. This model gives a reasonable description of closed shell molecules in the neighbourhood of their equilibrium geometry, but the method neglects the correlated movement of the electrons. One of the major undertakings of quantum chemistry the last 30 years has consequently been to develop schemes for obtaining an accurate description of electron correlation. With modern *ab initio* techniques the models are often of extremely high accuracy compared with experiment. For some properties the parameters derived from *ab initio* theory are even regarded as more accurate than the values obtained purely from experiment (e.g. nuclear quadropole moments [2]). One may predict that with even more powerful computers available in the future more and more chemical properties will be calculated with an accuracy so high that experiment will have to struggle hard to compete. Quantum chemical calculations may today also be performed for chemical species that can not be studied experimentally since they are extremely short lived, dangerous or unstable. Finally, it can be economically favourable to perform theoretical calculations instead of expensive experiments in the laboratory. This is especially useful for investigating trends or deciding between different solutions to a chemical problem. The last ten years many industrial and chemical companies have employed quantum chemists to perform molecular modelling with methods derived from *ab initio* quantum chemistry and other physical models.

1.1 Relativistic *ab initio* four-component calculations

One of the consequences of Einstein's theory of special relativity is the realization that particles can not travel faster than the speed of light, c. Particles moving at velocities close to the speed of light will have increased masses. The Schrödinger equation, however, does not take into account the effects of relativity correctly. One might say that the Schrödinger equation is more appropriate for a description of a universe where the speed of light is infinitely high. Already in 1929 a relativistically correct equation for electrons was developed by Dirac [3]. In this theory the scalar nonrelativistic wavefunction is replaced by a four-component entity, a four-spinor. Negative energy solutions which are connected with the existence of anti-particles are introduced as well The single-particle Dirac equation may be introduced in the quantum chemical models in the same way as the nonrelativistic Schrödinger equation, and the first relativistic mean-field calculations were performed by Swirles in 1934 [4]. The method is known as the Dirac–Hartree–Fock or Dirac–Fock method. The calculations were suggested to Swirles by Hartree while they were waiting at a London train station in 1934 [5]. Hence the author feels that the name Dirac–Hartree–Fock method is more appropriate.

The relativistic calculations based on the Dirac equation, four-component calculations, are significantly more expensive than nonrelativistic calculations based on the Schrödinger equation. This is the main reason why the Schrödinger equation was used almost exclusively for quantum chemical calculations until the late 1970's. For most of the

systems that one was studying the relativistic effects were small. The effects of relativity were small compared with the precision that was obtainable as well. However, the last decades it has been established that in molecules containing elements from the lower part of the periodic system relativistic effects are important. Close to the nuclei of heavy elements the electrons obtain relativistic velocities, and the description provided by the Schrödinger equation becomes inaccurate. In the limit $c \to \infty$ the Dirac equation effectively leads to results which are identical to those obtained from the Schrödinger equation. Relativistic effects may therefore be defined as anything arising from the finite speed of light, as compared to $c = \infty$ [6].

One of the most popular examples of a relativistic effect is that of the colour of gold (e.g., [6]). This colour is caused by the transition from the filled 5d band to the essentially 6s Fermi level. In a universe where the speed of light is infinitely high this transition corresponds to an absorbtion in the ultraviolet region giving gold the same colour as silver. However, relativity stabilizes the 6s band and lowers the transition energy such that the absorbtion enters into the visible region. This gives gold its characteristic colour. Relativity also changes the bonding in moleculs containing heavy elements. The unusual stability of the important Hg_2^{2+}-ion [6], the stability of the Au_2 bond [6] and the unexpected weakness of the bond in Pb_2 [7] are all examples of relativistic effects. These effects have been covered extensively in reviews [6–11]. In Paper IV of this thesis it is demonstrated that the chemical trends known as the lanthanide and actinide contractions have important contributions from relativistic effects. The actinide contraction is almost 50% larger than the lanthanide contraction, and this is a consequence of relativity.

There have been many studies of relativistic effects in structural chemistry both in fully relativistic calculations and in calculations based on one- and two-component approximations. The last years there has in addition been a growing interest in studing the effects of relativity on for example NMR properties, calculations of electric field gradients and parity-odd effects. These properties are dependent on the wavefunction in the nuclear region, and consequently the relativistic effects are expected to be very important. This assumption is confirmed by the few studies that have been performed, for example Papers I and II of this thesis on PT-odd effects in thallium fluoride.

The examples above show that relativistic methods must be employed in order to correctly explain many chemical and physical properties of heavy elements. The atomic Dirac–Hartree–Fock equations have traditionally been solved by finite difference methods. Calculations on molecules, however, are more efficiently performed if the wavefunctions are expanded in analytic basis sets in the spirit of Roothaan [12]. This method also has the advantage that a large number of virtual unoccupied orbitals are generated during the mean-field calculation. These may later be used in calculations to account for the effects of electron correlation.

The first four-component calculations employing basis set expansions experienced prob-

lems of 'variational collapse' ('finite basis set disease') and spurious solutions entering in the bound state spectrum. These and other effects were not previously known from nonrelativistic calculations, and they were believed to be connected with the negative energy spectrum. It was argued that bound state solutions should undergo a 'continuum dissolution' ('Brown–Ravenhall disease') as well, and that consequently four-component calculations for many electron systems were not possible in principle. Today, however, all these problems have been analysed and eliminated. This is discussed briefly in Sec. 3.1.1.

The initial problems with the four-component methods appear to have given the impression to many theoreticians that the fully relativistic methods not only were prohibitively expensive, but they were also plagued by various unhealthy 'diseases'. At least more work has been laid down in the development of one- and two-component approximations to the Dirac equation than in the development of the four-component methods. In this work the author will, however, focus on the fully relativistic methods based directly on the Dirac equation. The theoretical foundation of these methods is now on solid ground, and perhaps even more important, the usefulness and stability of the methods have been demonstrated in many applications, some of which are presented in this work. With the development of more powerful computers the fully relativistic four-component methods will undoubtedly become more popular in the future.

Several groups have the last ten years developed programs for Dirac–Hartree–Fock calculations on molecules [13–20]), The Dirac–Hartree–Fock method may be used to test the more approximate methods, and has been used to study bonding and properties of molecules containing heavy elements as well. Today, one of the most efficient codes are included in the DIRAC [21] program system. This program package has been developed in Oslo, mainly by T. Saue. The program employs direct methods that were pioneered by Almlöf, Fægri and Korsell [22] in Oslo in the 1980's, for the calculation of the two-electron integrals. The direct methods are characterized by the recalculation of integrals as they are needed, and one avoids heavy I/O and external memory bottlenecks. A great advantage is that advanced screening techniques may be used to reduce the computational cost. This makes the calculations not too expensive compared with nonrelativistic methods and one- and two-component approximations to the fully relativistic methods. All the relativistic molecular calulations presented in this work have been performed by the author with the DIRAC program system.

1.2 Outline of this thesis

An application of the Dirac–Hartree–Fock method in calculations on the thallium fluoride molecule is presented in Papers I and II of this thesis. The study represents one of the first fully relativistic four-component investigations of properties where the quality of the wavefunction in the highly relativistic region close to a heavy nucleus is tested.

In connection with this work it was necessary to determine which properties a basis set must have in order to give an accurate description of the molecular amplitudes in the neighbourhood of a heavy nucleus.

The second important topic of this work has been the implementation and application of efficient four-component direct Møller–Plesset second order perturbation theory (MP2). Details of the method and its implementation are given in Paper III together with applications on the coinage metal fluorides. Paper IV presents another application of the MP2 program in investigations on the lanthanide and actinide contraction. This is one of the first fully relativistic Dirac–Hartree–Fock and correlated studies of trends in the periodic system for a number of molecules with important relativistic effects. It is demonstrated that it is possible to perform correlated studies of trends of relevance for heavy element chemistry without the approximations inherent in methods with a less rigorous treatment of relativistic effects.

Chapt. 2 is a brief introduction to four-component calculations in molecules. Particular weight has been placed on topics relevant for this work. The advantages of the MP2 method and a brief introduction to the method is given in Sec. 2.8 and 2.9. Chapt. 3 deals with basis set experiments that were performed in order to study the quality of wavefunctions expanded in analytic basis sets close to a heavy nucleus. After a summary of the papers in Chapt. 4 a conclusion about the contributions of this thesis is given in Chapt. 5.

Chapter 2

The Dirac equation for atomic and molecular systems

2.1 The Dirac equation

The temporal development of a quantum system in nonrelativistic theory is given by the Schrödinger equation,

$$i\hbar\frac{\partial}{\partial t}\psi(\boldsymbol{r},t) = H\psi(\boldsymbol{r},t), \tag{2.1}$$

where the Hamiltonian operator, H, is obtained from the Hamiltonian function by replacing the position and momentum coordinates by their corresponding quantum mechanical operators. The relativistic Hamiltonian function for a free particle with rest mass m is

$$H = \sqrt{m^2c^4 + p^2c^2}, \tag{2.2}$$

and it is obvious that replacing the momentum coordinates with the momentum operators will give a Schrödinger equation where the time and position derivatives enter in a completely different fashion. The equation will not be invariant under a Lorentz transformation and can therefore not be the relativistic equation we are seeking in order to describe physical reality.

Dirac assumed that one might linearize the relativistic Hamiltonian,

$$\sqrt{m^2c^4 + p^2c^2} = c\left(\alpha_1 p_1 + \alpha_2 p_2 + \alpha_3 p_3 + \beta mc\right), \tag{2.3}$$

and obtained the first successful relativistic theory for electrons and other spin 1/2-particles [3]. The free-particle Dirac equation may be written in covariant form,

$$(\gamma^\mu p_\mu - mc)\psi = 0, \qquad p_\mu = i\hbar\frac{\partial}{\partial x^\mu}, \tag{2.4}$$

where there is an implied summation over the indexes $\mu = 0, \ldots, 3$. The position and time derivatives all enter in a symmetric manner in this equation, and since it meets the requirements of Lorentz invariance it is, unlike the Schrödinger equation, in agreement with Einstein's theory of special relativity. The 4×4 matrices in Eq. (2.4) satisfy anticommutation relations and Hermiticity conditions,

$$[\gamma^\mu, \gamma^\nu]_+ = 2g^{\mu\nu}, \qquad \gamma^{\mu\dagger} = \gamma^0\gamma^\mu\gamma^0. \tag{2.5}$$

Only the diagonal elements of the metric tensor, $g^{\mu\nu} = \mathrm{diag}(1, -1, -1, -1)$, are non-zero. Eq. (2.4) is satisfied for different representations of the γ^μ-matrices, but the most used representation in atomic and molecular physics is the standard representation, where we choose

$$\gamma^0 = \beta, \qquad \gamma^i = \beta\alpha_i, \tag{2.6}$$

and

$$\beta = \begin{pmatrix} I & 0 \\ 0 & -I \end{pmatrix}, \qquad \alpha_i = \begin{pmatrix} 0 & \sigma_i \\ \sigma_i & 0 \end{pmatrix}. \tag{2.7}$$

The σ_i-matrices are the 2×2 Pauli matrices that are well-known from electron spin theory,

$$\sigma_1 = \sigma_x = \begin{pmatrix} 0 & 1 \\ 1 & 0 \end{pmatrix}, \qquad \sigma_2 = \sigma_y = \begin{pmatrix} 0 & -i \\ i & 0 \end{pmatrix}, \qquad \sigma_3 = \sigma_z = \begin{pmatrix} 1 & 0 \\ 0 & -1 \end{pmatrix}. \tag{2.8}$$

and I is a 2×2 identity matrix. We obtain the free-particle Dirac equation in the time and space variables t and $\boldsymbol{r}$,

$$i\hbar\frac{\partial}{\partial t}\psi(\boldsymbol{r}, t) = H\psi(\boldsymbol{r}, t) = (c\boldsymbol{\alpha} \cdot \boldsymbol{p} + mc^2\beta)\psi(\boldsymbol{r}, t), \tag{2.9}$$

which is a set of four coupled first-order differential equations. The solutions $\psi_i(\boldsymbol{r}, t)$ are four-component entities, four-spinors, that have replaced the scalar wavefunctions in nonrelativistic theory. The probability density of a particle and the current entering in the continuity equation,

$$\partial^\mu j_\mu = \frac{\partial\rho}{\partial t} + \boldsymbol{\nabla} \cdot \boldsymbol{j} = 0, \tag{2.10}$$

are given by

$$\rho = \psi_i^\dagger(\boldsymbol{r}, t)\psi_i(\boldsymbol{r}, t), \quad \boldsymbol{j} = c\psi_i^\dagger(\boldsymbol{r}, t)\boldsymbol{\alpha}\psi_i(\boldsymbol{r}, t). \tag{2.11}$$

The term 'orbital' will be used for both scalar and four-component single-particle solutions in this work.

Introducing the vector of four-dimensional matrices

$$\boldsymbol{s} = \frac{\hbar}{2}\begin{pmatrix} \boldsymbol{\sigma} & 0 \\ 0 & \boldsymbol{\sigma} \end{pmatrix}, \tag{2.12}$$

it can easily be demonstrated that $\boldsymbol{s}$ represents the spin angular momentum of a spin 1/2-particle. Unlike nonrelativistic theory, the Dirac Hamiltonian does not commute

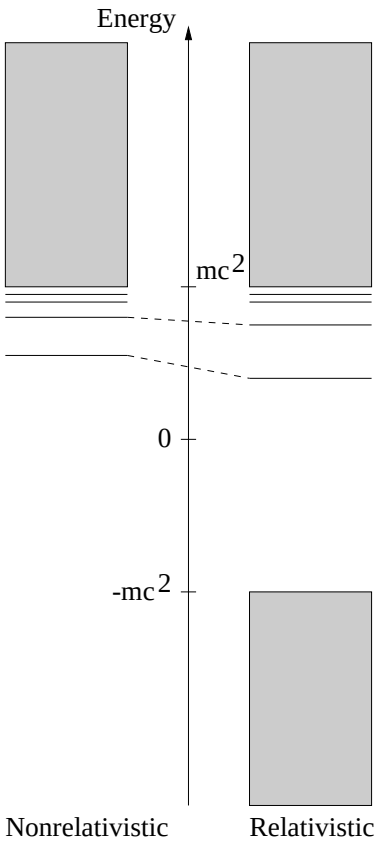

Figure 2.1: An illustration of the energy spectrum for a nonrelativistic and relativistic system. The main differences are the extra negative energy continuum in the relativistic case in addition to small energy changes in the bound state solutions.

with $\boldsymbol{s}$ or the orbital angular momentum operator $\boldsymbol{l}$, but it does commute with the total angular momentum $\boldsymbol{j} = \boldsymbol{l} + \boldsymbol{s}$. It is therefore seen that in the Dirac equation the spin enters as an integrated part of the general theory. It should be emphasized though, that despite the common *ad hoc* intoduction of spin in nonrelativistic theory spin is not a *consequence* of relativity. It may for example be introduced in nonrelativistic theory simply be replacing the kinetic energy operator $\boldsymbol{p}^2/2m$ by (e.g., [23])

$$T = \frac{1}{2m}(\boldsymbol{\sigma} \cdot \boldsymbol{p})(\boldsymbol{\sigma} \cdot \boldsymbol{p}). \tag{2.13}$$

Unlike the Schrödinger equation, the Dirac equation has both positive and negative energy solutions. For a free particle we have

$$E = \pm\sqrt{m^2c^4 + c^2p^2}, \tag{2.14}$$

and a spectrum that is symmetric with respect to zero. All the solutions are of continuum type and have energies above mc^2 or below $-mc^2$. The spectrum is not bounded from above or below. This is illustrated in Figure 2.1 where the rest energy of the particle, mc^2, has been added to the nonrelativistic energies in order to align the spectra. An external attractive potential introduces positive energy 'bound' states with energies in the gap below mc^2. One may discard the negative energy solutions in a classical theory since discontinous energy changes are not allowed. In quantum mechanics, however, this is not the case, and the positive energy solutions do not span a complete solution space for a general state.

Consequently, the relativistic theory introduces a new problem. The particles in the positive energy states should make rapid radiative transitions to the negative energy states. Contrary to nonrelativistic theory we do no longer have stable ground state solutions, and matter should not be stable. A massive reinterpretation of the theory is necessary, and Dirac's solution to the problem was his 'hole theory'. He assumed that in the physical world all the negative energy states are already filled with one particle, and transitions to them are forbidden by the Pauli exclusion principle. In this model the vacuum is the state where all the negative-energy levels are occupied by one particle. Additional particles must therefore be introduced in positive-energy levels.

This model also gives the possibility of explaining the anti-particle of the electron, the positron, as the 'hole' left behind when an electron is removed from the vacuum electron 'sea'. A high energy photon may excite an electron out of the vacuum into a positive energy state and leave a hole behind. The hole will be observed as the absence of a particle with energy $-E$ and charge $-e$, that is, a particle with energy E and positive charge e. The process described above is the creation of an electron–positron pair by a high energy photon. Dirac's relativistic theory made it possible to predict the existence of the positron, and it was a great success for the theory when this particle was observed for the first time in cosmic radiation by Anderson in 1933 [24]. The problem with the theory is that even one- or zero-(vacuum)particle problems become many-particle problems, and restricting oneself to particles only (electrons and holes) the number of particles may change during a process. The tool for such situations are field theories such as renormalized quantum electrodynamics (QED) which was developed in the 1940's by among others Feynman, Schwinger and Tomonaga. The extremely successful theory of QED is still too computationally demanding to handle general atomic and molecular systems. However, chemical energies are low compared to the rest energies of the particles, and the Dirac equation is sufficient for a precise treatment of atomic and molecular systems as long as one is not considering extremely accurate atomic structure calculations. The Dirac equation gives more accurate results than the Schrödinger equation for all chemical systems, but usually at a higher computational cost.

Interactions with external electromagnetic fields $\boldsymbol{E}$ and $\boldsymbol{B}$ which enter in the equations through the potential

$$A^\mu = (\phi/c, \boldsymbol{A}), \tag{2.15}$$

are included by invoking minimal electromagnetic coupling as in nonrelativistic theory. This involves the replacement

$$p^\mu \rightarrow p^\mu - qA^\mu. \tag{2.16}$$

We obtain the Dirac equation for an electron ($q = -e$) that interacts with nuclei, other electrons and other external fields

$$i\hbar\frac{\partial}{\partial t}\psi(\boldsymbol{r},t) = H\psi(\boldsymbol{r},t) = \left\{c\boldsymbol{\alpha}\cdot(\boldsymbol{p}+e\boldsymbol{A}(\boldsymbol{r},t)) + mc^2\beta - e\phi(\boldsymbol{r},t)\right\}\psi(\boldsymbol{r},t). \tag{2.17}$$

It may easily be showed (e.g., [25, 26]) that this equation gives the nearly correct gyromagnetic ratio, $g = 2$, in the relationship between the electron spin and the corresponding magnetic moment, $\boldsymbol{\mu}_s = -(ge\boldsymbol{s})/(2m)$. The exact value is approximately $g = 2.002319$ and may be calculated to extreme accuracy by QED.

The general four-spinor solutions of the Dirac equation, ψ_i, are written as

$$\psi_i = \begin{pmatrix} \psi_i^0 \\ \psi_i^1 \\ \psi_i^2 \\ \psi_i^3 \end{pmatrix} = \begin{pmatrix} \psi_i^{L\alpha} \\ \psi_i^{L\beta} \\ i\psi_i^{S\alpha} \\ i\psi_i^{S\beta} \end{pmatrix} = \begin{pmatrix} \psi_i^L \\ i\psi_i^S \end{pmatrix}. \tag{2.18}$$

The upper and lower two-spinors are usually denoted the upper and lower components, or large and small components for reasons to be explained later. The small component two-spinor is often given with an imaginary i written out explicitly as shown above. The reason for this is that with this notation the radial solutions for both the large and small components may be chosen to be real functions in atomic calculations. In molecular calculations the symmetry is lower, and both two-spinors are generally complex, something that will give higher computational demands compared with nonrelativistic calculations.

A time-independent Hamiltonian allows the separation of time and space variables as in nonrelativistic theory. The solutions of Eq. (2.17) may be written as

$$\psi_i(\boldsymbol{r},t) = \psi_i(\boldsymbol{r}) \times f(t), \quad \text{where } f(t) = \exp\left(-iE_it/\hbar\right). \tag{2.19}$$

Since we usually are most interested in the positive energy solutions of the Dirac equation the particle rest energy may be subtracted from the equation to align the spectrum with the solution spectrum of the Schrödinger equation. In a static potential $V(\boldsymbol{r}) = -e\phi(\boldsymbol{r})$ with no magnetic potential ($\boldsymbol{A} = 0$) this gives us the eqution that is the starting point of almost all molecular relativistic calculations, the energy eigenvalue equation or time-independent Dirac equation,

$$H\psi(\boldsymbol{r}) = \left\{c\boldsymbol{\alpha}\cdot\boldsymbol{p} + mc^2(\beta-1) + V(\boldsymbol{r})\right\}\psi(\boldsymbol{r}) = E\psi(\boldsymbol{r}). \tag{2.20}$$

This may be written out as two coupled differential equations for the two two-spinor components,

$$\begin{pmatrix} V(\boldsymbol{r}) - E & -i\hbar c(\boldsymbol{\sigma}\cdot\boldsymbol{\nabla}) \\ -i\hbar c(\boldsymbol{\sigma}\cdot\boldsymbol{\nabla}) & V(\boldsymbol{r}) - E - 2mc^2 \end{pmatrix} \begin{pmatrix} \psi^L(\boldsymbol{r}) \\ i\psi^S(\boldsymbol{r}) \end{pmatrix} = 0. \tag{2.21}$$

One may express the small component two-spinor in terms of the large component spinor as

$$\psi^S(\boldsymbol{r}) = \hbar c(V(\boldsymbol{r}) - E - 2mc^2)^{-1}(\boldsymbol{\sigma}\cdot\boldsymbol{\nabla})\psi^L(\boldsymbol{r}), \quad \text{or} \tag{2.22}$$

$$2c\psi^S(\boldsymbol{r}) = \left(\frac{V(\boldsymbol{r}) - E}{2c^2} - 1\right)^{-1}(\boldsymbol{\sigma}\cdot\boldsymbol{\nabla})\psi^L(\boldsymbol{r}), \tag{2.23}$$

where atomic units ($\hbar = e = m = 4\pi\epsilon_0 = 1$) have been used in the last step. Atomic units (a.u.) will be used in the rest of this work, but the parameters above may be written out explicitly where this is appropriate. For positive energy ('electron like') solutions the term $-2mc^2$ in Eq. (2.22) will dominate the other two terms in the denominator, and this justifies the description of ψ^L and ψ^S as the large and small components respectively. It should be noted that if the potential is high as for example close to heavy atomic nuclei, the upper and lower components may have amplitudes of the same order of magnitude. The fundamental theory of relativistic quantum mechanics has been covered extensively in textbooks [25–28].

2.2 Central field problems

The Dirac equation for atomic problems has been studied extensivly, and the basic theory is reviewed in textbooks on relativistic electron theory [25, 27, 29]. Here only a short summary that is relevant for this work is given. In the previous section it was mentioned that the zero potential system will only have solutions of scattering type for energies $E > mc^2$ and $E < -mc^2$. For an atomic system with nuclear charge Z we in addition have discrete bound state solutions in the gap $-mc^2 < E < mc^2$. These are the relativistic analogues of the nonrelativistic bound state solutions of the system (Figure 2.1). Within the mean-field approximation an electron is moving in the central field of the point or extended spherical nucleus and the mean-field of the other electrons. The single-particle bound state solutions are given by

$$\Psi(r,\theta,\varphi) = \frac{1}{r}\begin{pmatrix} P_{n,\kappa}(r)\chi_{\kappa,m_j}(\theta,\varphi) \\ iQ_{n,\kappa}(r)\chi_{-\kappa,m_j}(\theta,\varphi) \end{pmatrix}. \tag{2.24}$$

The spin–angular eigenfunctions are the two-spinors

$$\chi_{\kappa,m_j} = \frac{1}{\sqrt{2l+1}}\begin{pmatrix} a\sqrt{l+\frac{1}{2}+am_j}\,Y_l^{m_j-\frac{1}{2}}(\theta,\varphi) \\ \sqrt{l+\frac{1}{2}-am_j}\,Y_l^{m_j+\frac{1}{2}}(\theta,\varphi) \end{pmatrix}, \tag{2.25}$$

where $Y_l^{m_j}(\theta,\varphi)$ are spherical harmonics defined with the Condon and Shortley phase convention [30], and $a = 2(j-l) = \pm 1$ has the opposite sign of the quantum number κ.

Table 2.1: Angular part of s-, p- and d-type atomic four-spinors.

$sgn(m_j)$			$+$	$-$
l	κ	$\lvert m_j\rvert$		
0	-1	$1/2$	$\begin{Bmatrix} \begin{pmatrix} s \\ 0 \end{pmatrix} \\ \frac{1}{\sqrt{3}}\begin{pmatrix} -p_0 \\ \sqrt{2}p_1 \end{pmatrix} \end{Bmatrix}$	$\begin{Bmatrix} \begin{pmatrix} 0 \\ s \end{pmatrix} \\ \frac{1}{\sqrt{3}}\begin{pmatrix} -\sqrt{2}p_{-1} \\ p_0 \end{pmatrix} \end{Bmatrix}$
1	1	$1/2$	$\begin{Bmatrix} \frac{1}{\sqrt{3}}\begin{pmatrix} -p_0 \\ \sqrt{2}p_1 \end{pmatrix} \\ \begin{pmatrix} s \\ 0 \end{pmatrix} \end{Bmatrix}$	$\begin{Bmatrix} \frac{1}{\sqrt{3}}\begin{pmatrix} -\sqrt{2}p_{-1} \\ p_0 \end{pmatrix} \\ \begin{pmatrix} 0 \\ s \end{pmatrix} \end{Bmatrix}$
1	-2	$3/2$	$\begin{Bmatrix} \begin{pmatrix} p_1 \\ 0 \end{pmatrix} \\ \frac{1}{\sqrt{5}}\begin{pmatrix} -d_1 \\ 2d_2 \end{pmatrix} \end{Bmatrix}$	$\begin{Bmatrix} \begin{pmatrix} 0 \\ p_{-1} \end{pmatrix} \\ \frac{1}{\sqrt{5}}\begin{pmatrix} -2d_{-2} \\ d_{-1} \end{pmatrix} \end{Bmatrix}$
1	-2	$1/2$	$\begin{Bmatrix} \frac{1}{\sqrt{3}}\begin{pmatrix} \sqrt{2}p_0 \\ p_1 \end{pmatrix} \\ \frac{1}{\sqrt{5}}\begin{pmatrix} -\sqrt{2}d_0 \\ \sqrt{3}d_1 \end{pmatrix} \end{Bmatrix}$	$\begin{Bmatrix} \frac{1}{\sqrt{3}}\begin{pmatrix} p_{-1} \\ \sqrt{2}p_0 \end{pmatrix} \\ \frac{1}{\sqrt{5}}\begin{pmatrix} -\sqrt{3}d_{-1} \\ \sqrt{2}d_0 \end{pmatrix} \end{Bmatrix}$
2	2	$3/2$	$\begin{Bmatrix} \frac{1}{\sqrt{5}}\begin{pmatrix} -d_1 \\ 2d_2 \end{pmatrix} \\ \begin{pmatrix} p_1 \\ 0 \end{pmatrix} \end{Bmatrix}$	$\begin{Bmatrix} \frac{1}{\sqrt{5}}\begin{pmatrix} -2d_{-2} \\ d_{-1} \end{pmatrix} \\ \begin{pmatrix} 0 \\ p_{-1} \end{pmatrix} \end{Bmatrix}$
2	2	$1/2$	$\begin{Bmatrix} \frac{1}{\sqrt{5}}\begin{pmatrix} -\sqrt{2}d_0 \\ \sqrt{3}d_1 \end{pmatrix} \\ \frac{1}{\sqrt{3}}\begin{pmatrix} \sqrt{2}p_0 \\ p_1 \end{pmatrix} \end{Bmatrix}$	$\begin{Bmatrix} \frac{1}{\sqrt{5}}\begin{pmatrix} -\sqrt{3}d_{-1} \\ \sqrt{2}d_0 \end{pmatrix} \\ \frac{1}{\sqrt{3}}\begin{pmatrix} p_{-1} \\ \sqrt{2}p_0 \end{pmatrix} \end{Bmatrix}$
2	-3	$5/2$	$\begin{Bmatrix} \begin{pmatrix} d_2 \\ 0 \end{pmatrix} \\ \frac{1}{\sqrt{7}}\begin{pmatrix} -f_2 \\ \sqrt{6}f_3 \end{pmatrix} \end{Bmatrix}$	$\begin{Bmatrix} \begin{pmatrix} 0 \\ d_{-2} \end{pmatrix} \\ \frac{1}{\sqrt{7}}\begin{pmatrix} -\sqrt{6}f_{-3} \\ f_{-2} \end{pmatrix} \end{Bmatrix}$
2	-3	$3/2$	$\begin{Bmatrix} \frac{1}{\sqrt{5}}\begin{pmatrix} 2d_1 \\ d_2 \end{pmatrix} \\ \frac{1}{\sqrt{7}}\begin{pmatrix} -\sqrt{2}f_1 \\ \sqrt{5}f_2 \end{pmatrix} \end{Bmatrix}$	$\begin{Bmatrix} \frac{1}{\sqrt{5}}\begin{pmatrix} d_{-2} \\ 2d_{-1} \end{pmatrix} \\ \frac{1}{\sqrt{7}}\begin{pmatrix} -\sqrt{5}f_{-2} \\ \sqrt{2}f_{-1} \end{pmatrix} \end{Bmatrix}$
2	-3	$1/2$	$\begin{Bmatrix} \frac{1}{\sqrt{5}}\begin{pmatrix} \sqrt{3}d_0 \\ \sqrt{2}d_1 \end{pmatrix} \\ \frac{1}{\sqrt{7}}\begin{pmatrix} -\sqrt{3}f_0 \\ 2f_1 \end{pmatrix} \end{Bmatrix}$	$\begin{Bmatrix} \frac{1}{\sqrt{5}}\begin{pmatrix} \sqrt{2}d_{-1} \\ \sqrt{3}d_0 \end{pmatrix} \\ \frac{1}{\sqrt{7}}\begin{pmatrix} -2f_{-1} \\ \sqrt{3}f_0 \end{pmatrix} \end{Bmatrix}$

In this notation both the large and small component radial functions $P_{n,\kappa}(r)$ and $Q_{n,\kappa}(r)$ are real. The four-spinor $\Psi(r,\theta,\varphi)$ is a simultaneous eigenfunction of the operators j_z, j^2 and $\beta K = -\beta(2\boldsymbol{s}\cdot\boldsymbol{l}+1)$ with quantum numbers j, m_j and κ respectively. The principal quantum number is n as in nonrelativistic theory, and j and m_j denote the sum of the orbital and spin angular momentum, the total angular momentum, and its component along the z-axis. Only the total angular momentum is defined, and Ψ is no longer an eigenstate of the orbital $\boldsymbol{l}$ and the spin $\boldsymbol{s}$ angular momentum operators in relativistic theory. In Table 2.1 the angular part of the s-, p- and d-type four-spinors are given. Note that the densities depend on j and not l and that for example $s_{1/2}$ and $p_{1/2}$ four-spinors both have spherical densities and finite amplitudes at the nucleus. All spinors with $|\kappa| > 1$ have zero amplitudes at the nucleus in analogy with the corresponding orbitals in nonrelativistic theory. An important difference between nonrelativistic and relativistic theory is that the spin–orbit interaction between electron spin and orbital angular momentum is an integrated part of the theory. Each atomic shell with $l > 0$ is split up into two levels with positive and negative κ, related to l and j by

$$\kappa = 2(l-j)(j+1/2). \tag{2.26}$$

This is illustrated in Table 2.1 where the p- and d-shells have also been split into two levels with different κ-values equal to l and $-(l+1)$. For light atoms the spin–orbit splitting is small compared with the part of the electron–electron interaction that gives rise to the splitting of a configuration into terms. LS or Russell–Saunders coupling is appropriate, and the splitting of the atomic terms by spin–orbit coupling may be treated by perturbation theory. For heavy elements the spin–orbit interaction sometimes is the dominating interaction, jj coupling gives a more correct description and the fully relativistic methods will give the correct couplings which have to be introduced in other ways in methods based on one-component calculations.

2.3 Relativistic effects

Spin–orbit splitting is one of the main 'relativistic effects', the difference of a property calculated in relativistic and nonrelativistic theory. Briefly, the relativistic effects have three main consequences for the structural chemistry of heavy elements:

- Contraction and stabilization of s- and p-type orbitals and concurrent strengthening of bonds.
- Expansion of d- and f-type orbitals and concurrent weakening of bonds.
- Spin–orbit splitting of shells with $l > 0$. Contrary to the *ad hoc* introduction of spin in nonrelativistic theory, spin and spin–orbit coupling enter as a natural consequence of the equations in methods based on the Dirac equation.

It is demonstrated in the analysis of Schwarz et al. [31] and Baerends et al. [32] that all the atomic densities in one-electron systems are 'pulled in by the tail' and contracted in the relativistic case if compared with nonrelativistic calculations. The contraction is largest for the $s_{1/2}$- and $p_{1/2}$-spinors, and their contraction gives an increased screening of the nuclear charge in many-electron atoms causing an expansion of the spinors with zero amplitude at the nucleus. The trends can for example be seen from the tables of Desclaux [33], and in summary the effect of relativity is to contract and energetically stabilize the $s_{1/2}$- and $p_{1/2}$-spinors and to expand and destabilize d- and f-spinors. The $p_{3/2}$-spinors usually have the same radial extension as the nonrelativistic p-orbitals. All the relativistic effects scale roughly as Z^2. The relativistic effects in atoms are often used to explain the relativistic effects on molecular properties such as bond lengths, force constants and dissociation energies, but one must be careful when conclusions are drawn. As demonstrated by Ziegler et al. [34,35] and Snijders and Pyykkö [36] the large relativistic bond contraction in for example AuH may be explained by a diminished kinetic energy increase in the bonding region between the atoms in the relativistic case. They argue that the relativistic contraction of atomic spinors is a parallel effect, but not necessarily the cause of the bond contraction. Extensive reviews on relativistic effects in atoms and molecules have been given by Pyykkö [6, 8, 10, 11], Pitzer [9] and Balasubramanian [7].

2.4 Nuclear models

The differential equations for an atomic system are not well-defined without appropriate boundary conditions as Grant and Quiney have argued. In a basis set expansion of the wavefunction a basis that corresponds to the boundary conditions must be chosen. Grant and Quiney [37] demonstrate that the radial functions in Eq. (2.24) are asymptotically of the form $\exp(-\lambda r)$ for $r \to \infty$, where λ is real and positive for bound states. The boundary conditions at $r = 0$ depend on the nuclear model. Below different nuclear models that have been proposed are described.

In nonrelativistic theory the interactions between the electrons and nuclei have traditionally been described by the simple Coulomb interaction $V = -Z/r$, where r is the distance between an electron and the *point* nucleus with charge Z. All the orbitals in atoms have zero amplitude at the nucleus except for s-orbitals which have a cusp of the form $\sim \exp(-\alpha r)$. In relativistic calculations $s_{1/2}$- and $p_{1/2}$-spinors instead have a weak singularity at the nucleus [37]. This is purely an artifact of the point nuclear model, and it has become customary to use a more physically correct extended nuclear model, a finite nuclear model. This change the boundary conditions at the nucleus and give spinors which are essentially Gaussian in shape [38]. This is the case both for the large component of the $\kappa = -1$ spinors and the small component of the $\kappa = -1$ spinors. In molecular quantum chemistry and also sometimes in atomic calculations one expands the wavefunction in a large set of Gaussian basis functions. The convergence of ba-

sis sets of this type is much better with basis set size when the nuclear singularity is avoided [38, 39]. The only disadvantage of the extended nuclear model is that it introduces one or more new parameters in order to describe the nucleus and that calculated total energies are not directly comparable if different nuclear models have been used.

The measurement and calculation of nuclear structure has currently not reached the accuracy of modern atomic and molecular structure theory. Fortunately most of the properties one is interested in calculating in quantum chemistry will not depend strongly on the nuclear model employed. This may be seen from the success of nonrelativistic quantum chemistry where the unphysical point nucleus is used almost exclusively. The Fermi distribution (See e.g. [40]) is the model closest to the actual nuclear charge distribution, but the nuclear potential is difficult to write in closed form. It is not known to the author that this model has been used in molecular calculations. A simpler model is the uniform charged sphere model with the potential

$$\begin{aligned} V(r) &= -\frac{Z}{2R}(3-(r/R)^2), \quad r \leq R, \\ &= -\frac{Z}{r}, \qquad\qquad\qquad\quad r \geq R, \end{aligned} \tag{2.27}$$

where R is the nuclear radius. Matsuoka [41] has shown that the supposed difficulties with the nuclear attraction integrals for this model may simply be overcome in calculations employing Gaussian basis functions. The perhaps most popular model is the Gaussian charge distribution which was proposed by Visser et al. [42]. The nuclear distribution and potential are given by

$$\rho(r) = Z\left(\frac{\lambda}{\pi}\right)^{3/2} \exp\left(-\lambda r^2\right), \tag{2.28}$$

$$V(r) = -\frac{Z}{r}\mathrm{erf}(\sqrt{\lambda}r), \tag{2.29}$$

where $\mathrm{erf}(x)$ is the error function. The nuclear attraction integrals are very easy to implement since they are just modified two-electron integrals in a molecular program that uses Gaussian basis sets. The Gaussian nucleus also avoids the very unphysical discontinuity of the nuclear charge distribution at the boundary of the nucleus for the charged sphere model. A Gaussian nucleus has been used in all the calculations performed in this work.

For all the extended nuclear models the nuclear parameters are derived from experimental results or empirical formulas. The nuclear exponent for the Gaussian nucleus is for example chosen in such a way that the nuclear model has the same root-mean-square (rms) radius as the experimental value for the nucleus. Recently Visscher and Dyall [40] have published a set of recommended values for the nuclear parameters for the different nuclear models of the 109 first elements. It is advantageous if these parameters are used in relativistic calculations in the future. Total energies calculated by different methods may then be compared directly.

Table 2.2: Total Dirac–Hartree–Fock (DHF) energy for the Rn atom ($Z = 86$) for different nuclear models. The data are taken from Visscher and Dyall [40].

Nuclear model	Total DHF energy
Point	-23611.19283063
Uniform sphere	-23602.00551946
Fermi	-23602.02330712
Gaussian	-23602.10424554

For all the nuclear models the nuclear size is about five orders of magnitude smaller than the size of the atom. The rms value recommended by Visscher and Dyall [40] for Rn ($Z = 86$) is 1.0643×10^{-4} a.u. = 5.6 fm. The corresponding Gaussian nuclear exponent is 13.2424×10^{7} a.u. The rms value may be compared with the expectation value for the electron–nucleus distance, $\langle r \rangle$, for various spinors given by Desclaux [33]. For the most dense and diffuse spinors, the $1s_{1/2}$ and $6p_{3/2}$ spinors, $\langle r \rangle = 0.015$ and 2.58 a.u. respectively suggesting that for chemical properties where only the outer part of the valence spinors are important the choice of nuclear model will have no significant effect. However, for properties where the spinor amplitudes at or close to the nuclei are of importance the nuclear model may have large consequences, and one should avoid the unphysical point nucleus. In Figure 2.2 the radial amplitudes $P(r)/r$ and $Q(r)/r$ for the Dirac–Hartree–Fock $6s_{1/2}$ orbital of Rn have been plotted. Both the large and small component radial amplitude have been plotted as linear–linear and log–linear plots. As the figure illustrates, the wavefunctions for the point and Gaussian nucleus systems are identical, except in the nuclear region. At the center of the nucleus the point nuclear solution diverges, whereas the more physically correct Gaussian nucleus gives a smooth and continous wavefunction at the origin. We also note that the small component only gives a significant contribution to the density close to the nucleus. The highly localized small component density in Rn contributes only 0.63% to the total density, and the majority of this comes from the core-spinors [43].

The nuclear model is consequently not important for valence properties, but when comparing total energies one must be careful since the energies depend quite a lot on the nuclear model. This is illustrated by the Rn total energies [40] in Table 2.2. The difference in total energy is almost 10 a.u. between the point and finite nuclear models. Among the different finite nuclear models the energy differences are smaller but still significant. Unlike nonrelativistic calculations, the calculated energies will depend on the numerical value for the speed of light. To make direct comparisons of total energies between different programs Visscher and Dyall [40] recommend the value, $c = 137.0359895$ a.u., and this is the value used in the DIRAC program system and our version of GRASP [44, 45]. Surprisingly, it seems that there has been few cross-checks of the different atomic and molecular four-component programs. As a 'quality control', the author in the course of

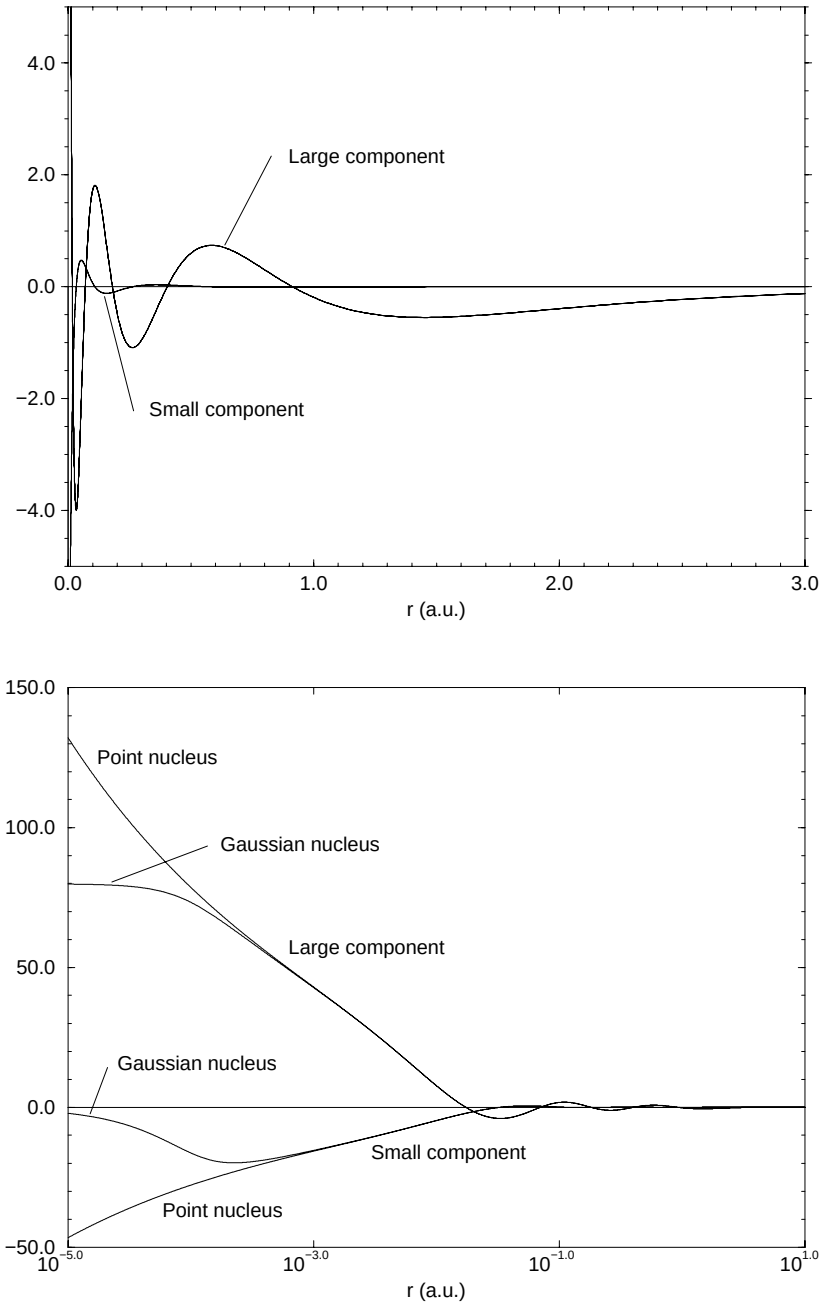

Figure 2.2: The radial wavefunction for the $6s_{1/2}$ spinor of Rn calculated within the Dirac–Hartree–Fock model with the GRASP program [44]. Both the point nucleus and Gaussian nucleus wavefunctions are plotted in the linear–linear and log–linear graphs. The root-mean-square radius of the atomic nucleus is 1.0643×10^{-4} a.u.

this work compared atomic calculations performed in DIRAC, the BERTHA program system [20,46] that has been developed in Oxford and the basis set version of GRASP. Molecular calculations have also been performed in DIRAC and BERTHA. All the test calculations agree to numerical accuracy.

The exact boundary conditions in molecular calculations are for all practical purposes identical to the boundary conditions in atoms. At large distances from the system the bound state amplitudes decay exponentially, and close to the nuclei the electric field is completely dominated by the spherical field of the nucleus. Well-behaved solutions also in molecular systems is therefore obtained if finite nuclei and sets of Gaussian atomic centered basis functions are employed.

2.5 The electron–electron interaction

In a system with more than one electron the electron–electron interaction must be introduced correctly as well. The instantaneous Coulomb electron–electron interaction is not Lorentz invariant, but the Lorentz invariant potential for the interaction may be derived from QED. Within this model the charged particles interact by emitting and absorbing virtual photons, and the formalism is most conveniently expressed in terms of perturbation theory and Feynman diagrams. The fully Lorentz invariant interaction can not be written in closed form, and as demonstrated by for example Grant and Quiney [37], the general potential for single photon exchange $V(\omega, r_{12})$ is dependent on the frequency of the exchanged photons and also on the electromagnetic gauge due to the truncation of the series expansion. For systems of electrons at chemical energies it is a good approximation to take the low frequency limit $\omega \rightarrow 0$, and for the interaction to lowest order in Coulomb gauge (transverse photon gauge, $\boldsymbol{\nabla} \cdot \boldsymbol{A} = 0$) one obtains,

$$\begin{aligned} V^C(0, r_{12}) &= \frac{e^2}{4\pi\epsilon_0 r_{12}} - \frac{e^2}{4\pi\epsilon_0 r_{12}} (\boldsymbol{\alpha}_1 \cdot \boldsymbol{\alpha}_2) + \frac{e^2}{8\pi\epsilon_0 r_{12}} \left(\frac{(\boldsymbol{\alpha}_1 \times \boldsymbol{r}_{12}) \cdot (\boldsymbol{\alpha}_2 \times \boldsymbol{r}_{12})}{r_{12}^2} \right) \\ &= \frac{e^2}{4\pi\epsilon_0 r_{12}} - \frac{e^2}{8\pi\epsilon_0 r_{12}} \left(\boldsymbol{\alpha}_1 \cdot \boldsymbol{\alpha}_2 + \frac{(\boldsymbol{\alpha}_1 \cdot \boldsymbol{r}_{12})(\boldsymbol{\alpha}_2 \cdot \boldsymbol{r}_{12})}{r_{12}^2} \right) \\ &= g^{Coulomb}(r_{12}) + g^{Breit}(r_{12}). \end{aligned} \tag{2.30}$$

The first term in this expression is the familiar Coulomb interaction and the second term the low-frequency limit of the Breit interaction. This operator was first postulated by Breit [47] who replaced the nonrelativistic velocity operator $\boldsymbol{v}_1$ by the relativistic operator $c\boldsymbol{\alpha}_1$ in the classical formula for the electron–electron interaction derived by Darwin [48]. In Lorentz gauge (Feynman gauge, $\boldsymbol{\nabla} \cdot \boldsymbol{A} + \frac{1}{c^2} \frac{\partial \phi}{\partial t} = 0$) the electron–electron interaction is given by

$$\begin{aligned} V^F(0, r_{12}) &= \frac{e^2}{4\pi\epsilon_0 r_{12}} - \frac{e^2}{4\pi\epsilon_0 r_{12}} (\boldsymbol{\alpha}_1 \cdot \boldsymbol{\alpha}_2) \\ &= g^{Coulomb}(r_{12}) + g^{Gaunt}(r_{12}), \end{aligned} \tag{2.31}$$

where the term added to the Coulomb interaction is known as the Gaunt term [49]. It has been demonstrated by Gorceix et al. [50] that the two potentials give different results in atomic calculations. Lindgren [51] has proven that only the Coulomb gauge potential is correct to second order in the fine structure constant ($\alpha = c^{-1}$), $\mathcal{O}(\alpha^2)$. The most correct procedure for including the terms of the electron–electron potential beyond the instantaneous Coulomb interaction is therefore to include the full Breit operator. The terms in the Coulomb gauge electron–electron potential beyond the frequency independent form are of the same order of magnitude as the self-energy and other QED effects [52] and will have minor effects on quantum chemical properties.

Bethe and Salpeter [29] warned against using the Breit and Gaunt interactions in any application other than first-order perturbation theory, but it is now known [52–54] that the analysis of Bethe and Salpeter is not applicable to the self-consistent-field procedure. The Breit (or Gaunt) operators may be included without problems in the Dirac–Hartree–Fock potential (introduced in Sec. 2.7).

Visser et al. [55] and Visscher et al. [56–58] have used the Gaunt term as an approximation to the full Breit term in Dirac–Hartree–Fock calculations. They found that the effect of including the Gaunt interaction was close to negligible for the calculated bond lengths, binding energies and force constants for PbH_4, PtH, the hydrogen halides and the halogen dimers. In studies of spin–orbit coupling in open-shell systems the Breit interaction is often important, but it is generally accepted that in molecular calculations electron correlation effects are usually much more important than going beyond the Coulomb interaction in the electron–electron potential.

2.6 The Dirac–Coulomb(–Breit) Hamiltonian

Relativistic quantum chemical calculations may be performed on the basis of the time-independent Dirac equation in Eq. (2.20) or on the basis of one- or two-component approximations. In this work we are mainly concerned with solving the fully relativistic Eq. (2.20) for molecular systems. We will work within the Born–Oppenheimer approximation and assume that the motion of the electrons and nuclei can be separated. Classically speaking, the electrons react instantaneously to the motion of the atomic nuclei since these are very heavy compared with the electrons. At any time the electrons are in an eigenstate in the potential of the static nuclei. This is a very simple and naive justification of the Born–Oppenheimer model, but a more rigorous derivation has been given by Born and Oppenheimer [59] and by Born and Huang [60] who analyzed the approximation by perturbation theory expansions. The most important consequence of the approximation is the potential energy surface concept where the electronic energy only enters as a potential in the effective Hamiltonian for the nuclear motion. This is both the computational and conceptual basis for molecular quantum chemistry and the link between quantum mechanics and the traditional chemical ball–and–stick picture

of a molecule. The Born–Oppenheimer approximation introduces very small errors in the quantum mechanical treatment, and corrections to the model may be introduced in the same fashion as in nonrelativistic theory [61]. When the nuclei are treated as static charges, a particular reference frame has been singled out. This destroys the symmetry of the fully Lorentz invariant equations, but the errors introduced are expected to be insignificant in calculations of chemical properties [62].

Within the Born–Oppenheimer approximation our goal is to solve the Dirac equation for the N_{occ} electrons of a molecule in the static field of N_{Nuc} nuclei. The Dirac–Coulomb(–Breit) Hamiltonian for a general system is given by

$$H_{DC(B)} = \sum_{i=1}^{N_{occ}} h_D(i) + \frac{1}{2} \sum_{i,j=1}^{N_{occ}\prime} g(i,j) \tag{2.32}$$

where the prime on the summation sign signifies that terms with index $i = j$ are not included in the sum. The one-particle operator $h_D(i)$ is identical to the operator in Eq. (2.20), where the external potential is caused by the presence of the nuclei,

$$h_D(i) = c\boldsymbol{\alpha}_i \cdot \boldsymbol{p}_i + mc^2(\beta_i - 1) + \sum_{K=1}^{N_{Nuc}} V_K(\boldsymbol{r}_i) \tag{2.33}$$

$$V_K(\boldsymbol{r}_i) = -\frac{Z_K}{\boldsymbol{r}_{iK}}, \tag{2.34}$$

and the potential is replaced by Eq. (2.29) when a Gaussian nuclear model is employed. The electron–electron interaction $g(i,j)$ is the instantaneous Coulomb interaction between the electrons i and j. For the Dirac–Coulomb–Breit Hamiltonian, the Breit term in Eq. (2.30) is also included. In the following the discussion will be restricted to the solution of the Dirac–Coulomb problem, but no extra difficulties apart from larger computational demands are introduced if the Breit operator is included. In the Born–Oppenheimer approximation the total energy of a molecular system also has a contribution from the interaction between the nuclei with charge Z_I,

$$V_{Nuc} = \frac{1}{2} \sum_{K,L=1}^{N_{Nuc}\prime} \frac{Z_K Z_L}{R_{KL}}, \tag{2.35}$$

which is treated classically.

2.7 The Dirac–Hartree–Fock method

In many areas of physics many-particle problems are solved by first generating a set of suitable single-particle solutions and then by using this basis to obtain approximate solutions for the full many-particle problem. This is also the approach that will be

used to solve the Dirac–Coulomb equation for atomic and molecular systems. The time independent many-particle Dirac–Coulomb equation is first solved,

$$H_{DC}\Psi(\boldsymbol{r}_1,\boldsymbol{r}_2,..,\boldsymbol{r}_N) = E\Psi(\boldsymbol{r}_1,\boldsymbol{r}_2,..,\boldsymbol{r}_N), \tag{2.36}$$

within what has become known as the Dirac–Hartree–Fock model. This method was pioneered by Swirles [4] in the 1930's, and the model is similar to the nonrelativistic Hartree–Fock model, but with the one-particle operators replaced by their relativistic analogues, Eq. (2.33). Both the Dirac–Hartree–Fock and Hartree–Fock models are independent-particle models where each electron is moving in the field of the nuclei and the average field of the other electrons. It is important to note that the Dirac–Coulomb equation, in the same way as the one-electron Dirac equation, is not bounded from below. This causes extra difficulties in the solution procedures unless precautions are taken. The wavefunction for a molecular or atomic closed-shell system Ψ is approximated by an anti-symmetrized Hartree-product (Slater determinant) of four-spinors,

$$\Phi(\boldsymbol{r}_1,\boldsymbol{r}_2,..,\boldsymbol{r}_N) = \mathcal{A}\left(\psi_1(\boldsymbol{r}_1)\psi_2(\boldsymbol{r}_2)\cdots\psi_N(\boldsymbol{r}_N)\right). \tag{2.37}$$

where $\mathcal{A}$ is an anti-symmetrization operator. Open-shell systems may be described by a sum of several Slater determinants, but we shall mostly be concerned with closed-shell systems in this work. In the Dirac–Hartree–Fock procedure the single-particle solutions are kept orthogonal, $\langle\psi_i|\psi_j\rangle = \delta_{ij}$, and determined variationally in the same way as for nonrelativistic calculations. We seek to make

$$E_{DHF} = \frac{\langle\Phi|H_{DC}|\Phi\rangle}{\langle\Phi|\Phi\rangle} \tag{2.38}$$

stationary, and obtain the one-particle Dirac–Hartree–Fock differential equations

$$F(\boldsymbol{r})\psi_i(\boldsymbol{r}) = \sum_{j=1}^{N_{occ}} \varepsilon_{ij}\psi_j(\boldsymbol{r}), \tag{2.39}$$

where the Fock operator is given by

$$F(\boldsymbol{r}) = h_D(\boldsymbol{r}) + u^{DHF}(\boldsymbol{r}). \tag{2.40}$$

The non-local single-particle Coulomb-exchange operator u^{DHF} is given by

$$\begin{aligned} u^{DHF}(\boldsymbol{r}_1)\psi_i(\boldsymbol{r}_1) &= \sum_{j=1}^{N_{occ}} \Big\{ \int \psi_j^\dagger(\boldsymbol{r}_2)\psi_j(\boldsymbol{r}_2)g(1,2)\psi_i(\boldsymbol{r}_1)d\boldsymbol{r}_2 \\ &\quad - \int \psi_j^\dagger(\boldsymbol{r}_2)\psi_i(\boldsymbol{r}_2)g(1,2)\psi_j(\boldsymbol{r}_1)d\boldsymbol{r}_2 \Big\}, \end{aligned} \tag{2.41}$$

and since this operator depends on the four-spinor solutions it is determined in an iterative way by a self-consistent-field (SCF) procedure. The Dirac–Hartree–Fock wavefunction is invariant to unitary transformations among the occupied spinors, but usually

one chooses to work with the set of solutions that diagonalizes the Fock matrix. This choice defines the canonical orbitals which have well-defined energies determined by the canonical Dirac–Hartree–Fock equations

$$\left\{h_D(\boldsymbol{r}) + u^{DHF}(\boldsymbol{r})\right\}\psi_i(\boldsymbol{r}) = \varepsilon_i\psi_i(\boldsymbol{r}). \tag{2.42}$$

Here ε_i are the Dirac–Hartree–Fock single-particle energy eigenvalues.

Compared with the nonrelativistic case extra complications occur since the Dirac–Coulomb operator is unbounded from below. It may naively be argued that one for this reason may obtain almost any energy for the system. However, since we are seeking to approximate bound electronic states, all the orthogonal single-particle spinors $\psi(\boldsymbol{r}_i)$ we use for describing this state must be taken from the bound state part of the positive energy spectrum. With this choice the Dirac–Coulomb operator is bounded from below as we do not allow electrons to enter into the negative energy states at all. As long as there is a clear separation between positive and negative energy states in the single-particle spectrum, the correct bound state for the system is obtained and the final optimized ground state will be the solution with the N_{occ} electrons occupying the N_{occ} lowest energy one-particle solutions of the positive energy spectrum. The energy expectation value for the Dirac–Hartree–Fock wavefunction is given by

$$\begin{aligned} E_{DHF} &= \sum_{i=1}^{N_{occ}}\langle\psi_i|h_D|\psi_i\rangle + \frac{1}{2}\sum_{i,j}^{N_{occ}}\left(\langle\psi_i\psi_j|g|\psi_i\psi_j\rangle - \langle\psi_i\psi_j|g|\psi_j\psi_i\rangle\right) && (2.43)\\ &= \sum_{i=1}^{N_{occ}}\varepsilon_i - \frac{1}{2}\sum_{i,j}^{N_{occ}}\left(\langle\psi_i\psi_j|g|\psi_i\psi_j\rangle - \langle\psi_i\psi_j|g|\psi_j\psi_i\rangle\right). && (2.44)\end{aligned}$$

Unlike nonrelativistic theory, spin symmetry can not be used to reduce the cost of the calculations. However, time reversal symmetry may be used to obtain some of the same savings that spin symmetry gives in the nonrelativistic case. The anti-unitary time reversal operator [63,64] is given by

$$\mathcal{K} = -i\begin{pmatrix}\sigma_y & 0\\ 0 & \sigma_y\end{pmatrix}\mathcal{K}_0, \tag{2.45}$$

where $\mathcal{K}_0$ is the complex conjugation operator. This operator commutes with the Dirac–Coulomb and the Dirac–Hartree–Fock operator in the absence of external magnetic fields. Usually interactions with magnetic fields may be introduced by perturbation theory, and time reversal symmetry may safely be exploited to gain computational savings. Due to time reversal symmetry the single-particle solutions for a closed-shell molecule come in degenerate pairs, Kramers pairs [64]. The relations between the two degenerate four-spinors in the pair, ψ and $\mathcal{K}\psi = \bar{\psi}$ are given by

$$\begin{aligned}\mathcal{K}(a\psi) &= a^*\mathcal{K}\psi && (2.46)\\ \mathcal{K}(\mathcal{K}\psi) &= \mathcal{K}\bar{\psi} = -\psi, && (2.47)\end{aligned}$$

where a is an arbitrary complex number. Note that since ψ and $\bar{\psi}$ are degenerate they may be rotated among each other and still be single-particle solutions of the Dirac–Hartree–Fock equations.

The atomic Dirac–Hartree–Fock equations are in practice two-point boundary value problems in the single radial coordinate, r, and may be solved by finite difference procedures (See e.g. [65]). The method gives solutions where the accuracy is limited only by the quality of the grid used in the numerical integrations. In practice, the solutions are the exact Dirac–Hartree–Fock solutions, the Dirac–Hartree–Fock limit. The finite difference atomic calculations in this work have been performed with a version of the GRASP program [44] which is also modified for basis set calculations [45]. The basis set module in GRASP has been written by K.G. Dyall.

The molecular Dirac–Hartree–Fock problem on the other hand, is generally a three-dimensional problem where numerical integration techniques are unwieldly. The method of expanding the single-particle solutions in a set of analytic basis functions has been adopted from nonrelativistic molecular theory where it was first introduced by Roothaan [12]. After the introduction of the basis set we obtain the matrix representation of the Dirac–Hartree–Fock equations. This is well suited for calculations on modern high-speed computers. The single-particle four-spinors are expanded in separate scalar function basis sets for the large $\{\chi^L\}$ and small $\{\chi^S\}$ component parts,

$$\psi_i = \begin{pmatrix} \psi_i^{L\alpha} \\ \psi_i^{L\beta} \\ \psi_i^{S\alpha} \\ \psi_i^{S\beta} \end{pmatrix} = \begin{pmatrix} \sum\limits_p \chi_p^L C_{pi}^{L\alpha} \\ \sum\limits_p \chi_p^L C_{pi}^{L\beta} \\ \sum\limits_q \chi_q^S C_{qi}^{S\alpha} \\ \sum\limits_q \chi_q^S C_{qi}^{S\beta} \end{pmatrix}. \tag{2.48}$$

Unlike nonrelativistic theory the expansion coefficients are generally complex. An imaginary factor i is often separated out of the small component coefficients as shown in Eq. (2.18). This is only useful in atomic calculations since both the large and small component coefficients then may be chosen to be real. A four-spinor expansion similar to Eq. (2.48) is used in the DIRAC program system, and a more detailed description is given in [21, 43]. An appealing feature of this procedure is that all the one- and two-electron integrals are over real scalar basis functions and may be calculated with existing integral codes from nonrelativistic molecular *ab initio* programs. The four-spinor solutions may also be expanded in sets of two-spinor basis functions, but this requires an integral package that can efficiently calculate integrals over these two-spinor basis functions. This is the procedure employed by Quiney et al. [20,66] in the BERTHA program system with very promising results.

The operators above have been given in first quantized form, but by involving second quantization techniques, we may use the single-particle solutions of the Dirac–Hartree–

Fock procedure as a basis and write the Dirac–Coulomb Hamiltonian as,

$$H_{DC} = \sum_{pq \in \{\varepsilon^+\}} h_{pq} p^\dagger q + \frac{1}{2} \sum_{pqrs \in \{\varepsilon^+\}} g_{prqs} p^\dagger q^\dagger sr, \tag{2.49}$$

where the matrix elements for the one- and two-electron operators are given by

$$h_{pq} = \langle \psi_p | h_D | \psi_q \rangle \tag{2.50}$$

$$g_{prqs} = \langle \psi_p \psi_q | g | \psi_r \psi_s \rangle = (pr|qs). \tag{2.51}$$

The operators $p^\dagger$ and p are the creation and annihilation operators of the four-spinor single-particle solution ψ_p. Note that we have truncated the summation to be over only positive energy single-particle solutions, $\{\varepsilon^+\}$. Grant and Quiney [37] have shown that this form of the Dirac–Coulomb operator gives the same solutions as the Hamiltonian operator derived from QED in Furry's bound state interaction picture [67] to the order $\mathcal{O}\left((Z\alpha)^2\right)$. The model is approximate as it neglects pair creation processes and radiative corrections such as vacuum polarization and self-energy, and it is commonly known as the no-pair or no virtual pair approximation. Going beyond this approximation one obtaines the Lamb shift (e.g., [28]) and other very small corrections for atoms and molecules with chemical energies. If they are needed these corrections may be introduced by standard perturbation theory procedures using the Dirac–Hartree–Fock solutions as the reference state. In this work, however, these terms will be neglected. The great advantage of Eq. (2.49) is that it has exactly the same form as the nonrelativistic Hamilton operator in second quantization. The same procedures for including electron correlation by for example many-body perturbation theory may therefore be used as in nonrelativistic theory.

There are a number of molecular Dirac–Hartree–Fock codes available (e.g., [13–19]), but perhaps the two most efficient are the DIRAC [21] and BERTHA [20] programs that have been developed in Oslo and in Oxford respectively. Both make extensive use of direct algorithms, where large integral classes are recalculated as they are needed. All the four-component molecular calculations that are presented in this work have been performed by the author with DIRAC. In this program molecular point group and time reversal symmetry is exploited in a quaternion formalism to reduce the computational cost [21, 43]. This formalism leads to a quaternion, complex or real Fock matrix depending on the point group symmetry of the problem. Advanced screening techniques are used to gain further savings. The cost of an SCF calculation scales as the fourth power of the number of basis functions of the system, N. Integral screening and other techniques may, however, be used to reduce the scaling to significantly less than the third power of N [68]. The author has implemented Pulay's direct inversion of the iterative subspace (DIIS) [69] in DIRAC as a part of this work [70]. This was necessary in order to increase the speed of convergence of the SCF procedure.

Papers I and II of this thesis describe Dirac–Hartree–Fock calculations performed by the author on thallium fluoride. These calculations employ very large Gaussian basis

sets satisfying the restricted kinetic balance prescription (Chapt. 3). The quality of the wavefunctions are close to the Dirac–Hartree–Fock limit in the neighbourhood of the thallium nucleus. PT-odd effects have been studied for which relativistic effects are dominating. This is one of the first investigations of the fully relativistic wavefunction in a molecule in the highly relativistic region close to a heavy nucleus. Nonrelativistic calculations give results which are in error by approximately a factor seven. The reader is referred to Papers I and II for further details.

2.8 Electron correlation

Löwdin defined the correlation energy for a system as the difference between the exact eigenvalue of the Hamiltonian and its expectation value in the Hartree–Fock approximation [71]. Methods going beyond the independent-particle model, which in relativistic theory will be the Dirac–Hartree–Fock model, are consequently referred to as correlated methods. It has been a major goal of molecular physics and quantum chemistry the last 30 years to develop efficient correlated methods. The Dirac–Hartree–Fock method is a useful starting point to approach a more correct description of the system. The complete spectrum of single-particle solutions obtained from the Dirac–Hartree–Fock procedure constitutes a one-particle basis from which one may construct determinants as in Eq. (2.37) and generate an N-particle basis $\{\Phi_i\}$. Wavefunctions for the system with higher accuracy may be written as a superposistion of N-particle determinants,

$$\Psi = \sum_i c_i \Phi_i. \tag{2.52}$$

In practice it is not possible to use complete one- and N-particle bases, and we seek to find approximations to the exact wavefunction in truncated spaces.

It has become customary to ascribe the shortcomings of the Dirac–Hartree–Fock wavefunction to two different sources, dynamical and nondynamical (static) correlation. Nondynamical correlation is connected with cases where the single determinant Dirac–Hartree–Fock wavefunction not even gives a qualitatively correct description of the full wavefunction. It is usually dealt with by multiconfigurational SCF (MCSCF) techniques or other multireference methods. It is most important in systems with near-degeneracies such as in studies of bond dissociation, open-shell systems and many transition metal compounds. Nondynamical correlation is usually not very important in closed-shell molecules close to the equilibrium geometry. Dynamical correlation is due to the shortcomings of the Dirac–Hartree–Fock wavefunction in description of the two-electron cusps correctly. The last five to ten years several groups have generated computer programs for relativistic correlated calculations, and a short summary is given below.

In the configuration interaction (CI) method one expands the N-electron wavefunctions as in Eq. (2.52) and optimizes the set of expansion coefficients. The first relativistic

four-component CI code was written by Visscher et al. [14, 56, 72] and incorporated in the MOLFDIR program package. It is prohibitively expensive not to truncate the CI expansion, and a good approximation is obtained by including in the expansion only determinants describing single and double excitations from the reference state (CISD). An important problem with truncated CI methods is that they are not size-extensive. This means that there is an incorrect scaling of the correlation energy of a system with the number of particles, and this may give important errors for systems with many electrons. For this reason there has been a large interest in size-extensize methods, especially coupled-cluster methods. The most popular are coupled-cluster calculations with single and double excitations (CCSD), and CCSD with triple excitations treated perturbatively, CCSD(T). In addition to being size-extensive, the coupled-cluster methods usually give a better approximation to the correlation energy at a lower cost than CI methods. Relativistic coupled-cluster programs have been developed by Kaldor and Eliav [73] and by Visscher et al. [74], and give impressive results. This is especially the case for many of the atomic coupled-cluster calculations where large basis sets may be used without too high computational demands (e.g., [75]). A major problem with the molecular systems is that one necessarily has to truncate the one-electron basis to reduce the size of the problem due to the quite substantial amount of work involved in the calculations. Especially the four-index transformation of two-electron integrals from atomic centered to molecular orbitals is very expensive in four-component calculations.

The coupled-cluster methods are (at least in the most common formulations) single reference methods, and even if at least the CCSD(T) method may account for surprisingly much of the nondynamical correlation, systems with severe near-degeneracy problems should be treated by multireference CI [14, 72] or MCSCF. Currently there are no efficient relativistic four-component MCSCF programs available. However, algorithms have been derived by Dyall et al. [76], and a program is under development [77] for inclusion in the BERTHA program system [20].

Many-body perturbation theory with the Dirac–Hartree–Fock wavefunction as the reference may be used to calculate the correlation energy to high accuracy in systems with little nondynamical correlation. In quantum chemistry the most popular approach is Møller–Plesset perturbation theory [78] where the second-order energy contribution is referred to as the MP2 energy. The method has gained widespread use. Higher order contributions are the MP3, MP4, and so on, energies, but experience has shown that coupled-cluster methods are more efficient for obtaining accurate results. The MP2 energy on the other hand, has the advantage that it is the simplest and least expensive useful correlated method. Dyall has derived algorithms for four-component relativistic MP2 [79] both for open- and closed-shell systems. In this work the author has continued this work and written an efficient integral-driven direct MP2 program which is described in Paper III. It has been integrated in the DIRAC program system [21].

The scaling of the cost of a method is often expressed in powers of N, where N is the size of the system given by the number of basis functions used in the expansion of the

wavefunction. Compared with the Dirac–Hartree–Fock method which scales as N^4, all the correlated methods have a steeper scaling with N. The first step in coupled-cluster, CI and MPn calculations is a four-index transformation of the two-electron integrals from atomic-orbital to molecular-orbital basis,

$$(ij \mid kl) = \sum_{XY} \sum_{\sigma\gamma} \sum_{pqrs} C_{pi}^{X\sigma^*} C_{qj}^{X\sigma} C_{rj}^{Y\gamma^*} C_{sb}^{Y\gamma} (pq \mid rs), \tag{2.53}$$

where X and Y runs over *Large* and *Small* and σ, γ denote α, β. Within the no-pair approximation $i, j, \ldots$ runs over *positive energy* spinors that are either occupied or unoccupied (virtual spinors). The four-index transformation is performed as four successive one-index transformations. If the number of molecular orbitals is N', the four transformations scale as $N'N^4$, N'^2N^3 and so on.

In nonrelativistic calculations the number of molecular orbitals is often almost as large as N, and a scaling of N^5 is an appropriate description of the cost that is involved in the transformations. For relativistic calculations, however, N' is often just a small fraction of N. All the negative energy solutions are excluded, and also a large fraction of the core electrons and high energy virtual orbitals may be neglected. This is at least the case for calculations of valence properties where the correlation of the core is not important. Consequently, the N'^4 two-electron integrals over molecular orbitals constitute a much smaller set than the integrals over atomic centered basis functions. The four-index transformation is therefore the most expensive step in the correlated calculation, and when it has been performed, the actual calculation of the correlation energy is cheap. Relativistic CCSD, CCSD(T) or MP3 calculations will consequently not have very different cost since for all these methods the same four-index transformation dominates. However, the MP2 method has the advantage that it does *not* use the full class of N'^4 integrals. Only the much smaller class of $N_o^2 N_v^2$ integrals is needed, where N_o is the number of occupied and N_v the number of virtual orbitals ($N' = N_o + N_v$). In a typical calculation (e.g., Paper IV) N_o is of the order 25 and N_v of significantly more than one hundred. The most expensive and dominating step in the MP2 calculation is the first step in the four-index transformation. The cost is $N_o N^4$ and in practice not much more than several Dirac–Hartree–Fock iterations.

2.9 Second-order Møller–Plesset perturbation theory

In Møller–Plesset perturbation theory [78,80] one chooses the operator

$$H_0 = \sum_{pq} \langle \psi_p | h_D + u^{DHF} | \psi_q \rangle p^\dagger q = \sum_p \varepsilon_p p^\dagger q \tag{2.54}$$

as the operator of the unperturbed system. The perturbation is given by

$$V = \frac{1}{2}\sum_{pqrs}\langle\psi_p\psi_q|g|\psi_r\psi_s\rangle p^\dagger q^\dagger sr - \sum_{pq}\langle\psi_p|u^{DHF}|\psi_q\rangle p^\dagger q, \tag{2.55}$$

and consequently the full operator of the system including electron correlation is

$$H = H_0 + V, \tag{2.56}$$

identical to the operator in Eq. (2.49). Using ordinary Rayleigh–Schrödinger perturbation theory it is elementary to show (e.g., [81]) that the zeroth- and first-order energy corrections are

$$E^{(0)} = \sum_i^{N_{occ}} \varepsilon_i, \tag{2.57}$$

$$E^{(1)} = -\frac{1}{2}\sum_{i,j}^{N_{occ}} \left(\langle\psi_i\psi_j|g|\psi_i\psi_j\rangle - \langle\psi_i\psi_j|g|\psi_j\psi_i\rangle\right), \tag{2.58}$$

and it is seen from Eq. (2.44) that in Møller–Plesset theory the Dirac–Hartree–Fock energy is given by the sum of these two terms,

$$E_{DHF} = E^{(0)} + E^{(1)}. \tag{2.59}$$

The lowest order correction to the Dirac–Hartree–Fock energy is the second-order Møller–Plesset energy correction, the MP2 energy, given by

$$E^{(2)} = \frac{1}{4}\sum_{ij}^{N_{occ}}\sum_{ab}^{N_{virt}} \frac{|\,(ia\mid jb) - (ib\mid ja)\,|^2}{\varepsilon_i + \varepsilon_j - \varepsilon_a - \varepsilon_b} = \frac{1}{4}\sum_{ij}^{N_{occ}}\sum_{ab}^{N_{virt}} \frac{|< ij \parallel ab >|^2}{\varepsilon_i + \varepsilon_j - \varepsilon_a - \varepsilon_b}, \tag{2.60}$$

where i and j are occupied four-spinors and a and b runs over the N_{virt} unoccupied spinors. Starting with the Furry representation of QED it may be demonstrated [20,82] that E_{DHF} in Eq. (2.59) is correctly obtained with additional Lamb shift and Breit contributions. To second order, however, QED gives in addition to the expression in Eq. (2.60) a second term

$$E^{(2)}_{-} = -\frac{1}{4}\sum_{ij}^{N_{occ}}\sum_{rs}^{N^-} \frac{|< ij \parallel rs >|^2}{\varepsilon_i + \varepsilon_j - \varepsilon_r - \varepsilon_s}, \tag{2.61}$$

where r and s runs over negative energy states. This term stems from a correction of the correlation energy from the negative energy 'sea'. Quiney et al. [83] have shown that this term gives contributions of the order $\mathcal{O}((Z\alpha)^4)$, and that it may safely be neglected in calculations of chemical properties.

In Paper III of this thesis the implementation of Kramers restricted MP2 is summarized. The method has been implemented by the author in a direct formalism for closed-shell

systems. The two-electron integral relations

$$\begin{array}{rclrcl} (ia \mid jb)^* &=& (\bar{i}\bar{a} \mid \bar{j}\bar{b}), & (i\bar{a} \mid j\bar{b})^* &=& (\bar{i}a \mid \bar{j}b), \\ (ia \mid \bar{j}\bar{b})^* &=& (\bar{i}\bar{a} \mid jb), & (i\bar{a} \mid \bar{j}b)^* &=& (\bar{i}a \mid j\bar{b}), \\ (i\bar{a} \mid jb)^* &=& -(\bar{i}a \mid \bar{j}\bar{b}), & (ia \mid j\bar{b})^* &=& -(\bar{i}\bar{a} \mid \bar{j}b), \\ (i\bar{a} \mid \bar{j}\bar{b})^* &=& -(\bar{i}a \mid jb), & (ia \mid \bar{j}b)^* &=& -(\bar{i}\bar{a} \mid j\bar{b}), \end{array} \tag{2.62}$$

have been used. The relations are derived using the definitions in Eq. (2.46), and p and $\bar{p}$ are the two spinors in a Kramers pair. After substitution of these expressions into Eq. (2.60) and some tedious algebra, one obtains the expression for the Kramers restricted MP2 energy

$$\begin{aligned} E^{(2)} &= \frac{1}{2}\sum_{j\le i}^{N_{occ}/2}\sum_{b\le a}^{N_{virt}/2}\frac{(2-\delta_{ij})(2-\delta_{ab})}{\varepsilon_i+\varepsilon_j-\varepsilon_a-\varepsilon_b}\Big(|<ij||ab>|^2+|<\bar{i}j||ab>|^2 \\ &+|<i\bar{j}||ab>|^2+|<ij||\bar{a}b>|^2+|<ij||a\bar{b}>|^2 \\ &+|<i\bar{j}||a\bar{b}>|^2+|<ij||\bar{a}\bar{b}>|^2+|<i\bar{j}||\bar{a}b>|^2\Big), \end{aligned} \tag{2.63}$$

or equivalently

$$\begin{aligned} E^{(2)} &= \frac{1}{2}\sum_{ij}^{N_{occ}/2}\sum_{ab}^{N_{virt}/2}\frac{1}{\varepsilon_i+\varepsilon_j-\varepsilon_a-\varepsilon_b}\Big(|<ij||ab>|^2+|<ij||\bar{a}\bar{b}>|^2 \\ &+2|<i\bar{j}||a\bar{b}>|^2+2|<i\bar{j}||ab>|^2+2|<ij||a\bar{b}>|^2\Big). \end{aligned} \tag{2.64}$$

Eq. (2.63) is the expression that is used to calculate the MP2 energy in DIRAC. However, as noted earlier, the actual calculation of the MP2 energy is much less than 1% the cost of the four-index transformation.

In the nonrelativistic limit ($c \to \infty$) the expression reduces to[1]

$$E^{(2)} = \sum_{ij}^{N_{occ}/2}\sum_{ab}^{N_{virt}/2}\frac{(ia|jb)(2(ai|bj)-(bi|aj))}{\varepsilon_i+\varepsilon_j-\varepsilon_a-\varepsilon_b}. \tag{2.67}$$

[1]It is always possible to transform degenerate spinors to a set of spinors that are pure spin α- and β-spinors in the nonrelativistic limit . With this choice densities $(i\bar{j}) = (i^\alpha j^\beta)$ with an odd number of bars (β-spin) give no contributions due to spin orthogonality. This leaves us with a simplified Eq. (2.64),

$$E^{(2)} = \frac{1}{2}\sum_{ij}^{N_{occ}/2}\sum_{ab}^{N_{virt}/2}\frac{1}{\varepsilon_i+\varepsilon_j-\varepsilon_a-\varepsilon_b}\left(|<ij||ab>|^2+|<ij||\bar{a}\bar{b}>|^2+2|<i\bar{j}||a\bar{b}>|^2\right), \tag{2.65}$$

where we have

$$\begin{array}{rcl} |<ij||ab>|^2 &=& |(ia|jb)-(ib|ja)|^2, \\ |<ij||\bar{a}\bar{b}>|^2 &=& |(i\bar{a}|j\bar{b})-(i\bar{b}|j\bar{a})|^2 = 0, \\ |<i\bar{j}||a\bar{b}>|^2 &=& |(ia|\bar{j}\bar{b})-(i\bar{b}|\bar{j}a)|^2 = |(ia|jb)|^2. \end{array} \tag{2.66}$$

Inserting this in Eq. (2.65) we obtain Eq. (2.67).

The relativistic expression is more complicated due to the larger number of non-zero contributions. In addition the integrals in general are complex, and the integral symmetry is reduced. However, point group symmetry have been employed to reduce the cost of the calculations in the new version of the MP2 program that have been used for the work presented in Paper IV. For the real groups (D_2, D_{2h} and C_{2v}) all the integrals in Eq. (2.63) are real, and the 'odd-bar' integrals are all zero. In the complex groups (C_s, C_2 and C_{2h}) the integrals are complex, but the 'odd-bar' integrals are still zero. It is only for the quaternion groups (C_1 and C_i) that all the integrals in Eq. (2.63) have to be calculated. The new direct MP2 scheme that employs point group symmetry and a quaternion formalism has been implemented in DIRAC program system [21] by the author. However, the theory and parts of the new four-index transformation have been developed in cooperation with L. Visscher and T. Saue. The new algorithms will be presented elsewhere [84].

Chapter 3

Basis sets and kinetic balance

The four-spinor wavefunction is usually parametrized in molecular calculations by expanding the single-particle solutions in a set of analytic basis functions (e.g., Eq. (2.48)). The choice of basis set is almost exclusively given by a set of atomic centered Slater or Gaussian functions. Gaussian basis sets have become particularly popular. With this choice, the most time-consuming integrals in molecular calculations, the two-electron integrals, can be calculated extremely efficiently. The use of Gaussian basis sets was pioneered by Boys [85], and the highly sophisticated algorithms for the calculation of integrals over Gaussian functions have recently been reviewed by Helgaker and Taylor [86]. In the DIRAC program system [21] scalar Gaussian basis sets are employed, and the integrals are calculated with the HERMIT [87] program. HERMIT is now a part of the DALTON program system [88].

There is an abundance of Gaussian basis sets available for the lighter elements. Fewer basis sets have been published for the heavy elements in the lower part of the perodic system. In this course of this work a number of basis sets have been optimized for heavy elements [89]. An energy-optimized dual family basis set[1] for thallium is given in Paper II. Basis sets of similar quality for the coinage metals are given in Paper III. Finally, in Paper IV, energy-optimized basis sets for lanthanum, lutetium, actinium and lawrencium are reported. In Papers I and II even-tempered basis sets have been used as well. The exponents of these basis sets are defined by the prescription

$$\lambda_i = \alpha\beta^{i-1}, \quad \text{where} \quad i = 1, 2, .., N. \tag{3.1}$$

Here α defines the most 'diffuse' function in the basis set and β is a parameter related to the 'density' of functions in the basis set (Low β gives high density). In the limit

[1] The term 'dual family basis set' will be used for sets where the d-function exponent set is a subset of the s-function exponent set, and there is a relationship of this type between the f- and p-functions as well. The reasons for choosing basis sets of this type will become clear in Sec. 3.1.3. In 'family basis sets' the exponents for all angular quantum numbers are selected from the same master list.

$N \rightarrow \infty$ a complete basis may in principle be obtained if both α and β are allowed to vary with N [90].

The same basis sets are applicable in nonrelativistic calculations and for the large components in four-component calculations. The basis sets described above are of this 'large component' type. In four-component calculations, also the small component wavefunction is expanded in a finite basis. The choice of this basis set is closely connected with the concept of kinetic balance. This will be discussed in the next section.

In Papers I and II of this work we report one of the first fully relativistic four-component investigations of properties where the pointwise accuracy of the molecular amplitudes in the neighbourhood of a heavy nucleus is critically tested. One of the parameters that have been calculated is proportional to the gradient of the electron density at the center of the thallium nucleus. It is well-known that properties of this type are notoriously difficult to calculate in nonrelativistic theory. In a four-component procedure where both the large and small component of the wavefunction contribute to the density, the calculations are not expected to be simpler. Earlier basis set investigations of the quality of the wavefunction in the nuclear region have concentrated on average properties such as energy eigenvalues and expectation values like for example $\langle r \rangle$ or $\langle r^1 \rangle$. Such properties may have excellent values and at the same time the actual amplitudes at each point in space may have large errors. A wavefunction with large 'wiggles' may for example in average give a density that is a good approximation to the correct wavefunction. In Sec. III.B of Paper II the parameter $(p_0/q_0)^\kappa$, that is (p_0/q_0) to the power of κ, has been described. This ratio provides a test for the pointwise accuracy of the amplitudes at the center of the nucleus. It is expected and also demonstrated in Paper II that this ratio is much more sensitive to the basis set parameters than the expectation value properties. By performing the power series expansion in Sec. III.B of Paper II to second order one may calculate [91] the exponent for the essentially Gaussian shaped amplitudes in the nuclear region of a heavy nucleus. For the thallium $\kappa = +1$ spinors this exponent is 1.066×10^7. In this chapter a summary is reported of basis set experiements that have been performed in order to investigate the convergence with basis set size of the amplitudes in the neighbourhood of a heavy nucleus. A brief introduction to the concept of kinetic balance is given in Sec. 3.1.1. The two versions of kinetic balance, restricted (RKB) and unrestricted kinetic balance (UKB) are discussed in Sec. 3.1.2, and the implementation of RKB in DIRAC is described in Sec. 3.1.3. Sec. 3.2 is a summary of the basis set experiments. A few 'rules' for the generation of basis sets that give correct amplitudes in the nuclear region are given in Sec. 3.3.

3.1 Kinetic balance

3.1.1 Variational collapse

The first relativistic four-component basis set calculations were plagued by various problems that were not known from nonrelativistic calculations (e.g., [92,93]). In calculations both on one- and many-electron systems one found that the energies of the bound electrons could be much lower than the exact energies. An unconstrained optimization of the basis set parameters could give bound states plunging into the negative energy continuum, and negative energy solutions entered into the gap above $-mc^2$ as intruder states. Unlike the experience that one had from nonrelativistic calculations, it was difficult to make the energies converge towards the exact energies as the basis set was increased. The problems were termed 'variational collapse' or 'finite-basis set disease'. In 1984 Kutzelnigg [94] summarized the proposals to overcome these problems and gave a detailed review of about 15 to 20 different approaches to the problem. Among them were transformations of the Dirac operator in various ways to two-spinor form, manipulations of the matrix representations of the operator and the replacement of the Dirac operator by bounded operators, for example its square. Many of these procedures have later been applied with success. In this present work, as well as in most other four-component approaches to relativistic calculations, the variational collapse problems are solved by a special choice of basis set.

McLean and Lee [13] and Ishikawa et al. [95] observed that in calculations where the large component basis set was given by $\{\chi\}$, a small component basis set that included $\{(\boldsymbol{\sigma}\cdot\boldsymbol{p})\chi\}$ led to variational stability. Stanton and Havriliak [96] termed this choice of basis set 'the kinetic balance principle', and showed that finite basis set calculations with kinetically balanced basis sets will not give severe variational collapse. They also demonstrated that the bounds are not rigorous, but that energy eigenvalues might drop below exact energies by an amount of the order $1/c^4$. In the limit of a complete basis set this error is expected to disappear, and this is also the experience from practical calculations. Schwarz and Wallmeier [93] analyzed the variational collapse problem and showed that it was caused by a shortfall in the kinetic energy. This occurs due to an incorrect coupling of the large and small component in basis sets that does not have the correct kinetic balance. The choice of a kinetically balanced basis also ensures that in the limit $c \to \infty$ the relativistic energy eigenvalues approach the eigenvalues of the Schrödinger equation in the same basis. Dyall, Grant and Wilson [97] approached the problem of kinetic balance as one of representations of operator products in finite bases. Quiney et. al [37,53,98] have emphasized the importance of the boundary conditions on the problem. They have shown that the kinetic balance prescription is a necessary but not sufficient condition to avoid variational collapse. In atomic calculations the basis functions must also fulfill the boundary conditions of the atomic problem at $r \to \infty$ and $r = 0$. As most basis sets are of exponential function type and has the correct

behavior at large distances from the nucleus, it is especially the last condition that might cause problems. Special care must be taken for point nucleus calculations [20, 37]. However, for extended nuclei the non-zero four-spinor amplitudes in the nuclear region are essentially Gaussian in shape [38]. The choice of atomic centered Gaussian basis functions for computational gains thus yields an added advantage since this basis set automatically fulfills the boundary conditions at the nucleus. The analysis is also applicable in the molecular case since there is an exponential decay of the wavefunction at large distances from the molecule. Close to a nucleus the central field of the nucleus dominates completely and gives rise to the same Gaussian shape of the amplitudes as in the atomic case. In many-electron mean-field Dirac–Hartree–Fock calculations the solutions are of single-particle type just as in the one-electron case. The extra contribution to the potential from the mean-field at the nucleus is tiny. Consequently exactly the same analysis and conclusions about variational stability may be applied in the two cases. Talman [99] has studied the solution procedure of the Dirac equation as a minimax problem. This also has given an increased understanding of the nature of the variational collapse problem.

A many-electron system in a bound state configuration is degenerate with an infinite number of configurations where electrons are occupying positive and negative energy continuum states. It has been argued that a many-particle bound configuration thus should be 'dissolved' in continuum states. This 'continuum dissolution' or 'Brown–Ravenhall disease' was first described by Brown and Ravenhall [100] and more recently be Sucher [54]. Sucher [54] and Mittleman [101] have argued that the electron-electron interaction operators should be surrounded by projection operators that project onto positive energy solutions. Within the Dirac–Hartree–Fock model this is done in practice by vector selection since electrons only are allowed to occupy positive energy states. This corresponds to mean-field projectors within the Furry picture of QED. The Dirac–Hartree–Fock procedure generates solutions of single-particle type, and one is never solving the full many-body equations variationally. Many-body effects may later be introduced by, for example, many-body perturbation theory. This is done within the no-pair approximation in a second quantization based approach (e.g., [20,37]). Within this scheme, continuum dissolution can occur neither in the Dirac–Hartree–Fock procedure nor in the subsequent correlated calculation.

In summary, kinetically balanced basis sets give energy eigenvalue spectra for molecular and atomic systems that consist of continuum solutions below $-mc^2$ and above mc^2, as well as bound state solutions in the gap below mc^2. There is a strict separation of positive and negative energy states for any reasonble chemical system, and the electrons of the system are allowed to occupy only positive energy states. The calculated energies converge towards the exact solutions when the basis set is increased towards completeness. The convergence may be from above or below, and this is the only difference from the nonrelativistic case. In this sense the Undheim-Hylleraas-Macdonald theorem [102] is not satisfied. In practical calculations, however, with reasonable choices of basis sets the energies almost exclusively approach the exact solutions from above. Some researchers

feel uncomfortable with the fact that the Undheim–Hylleraas–Macdonald theorem is not strictly satisfied, and that there are no strict lower bounds for the energies. However, this causes no problems that are not present in for example many-body perturbation theory and coupled cluster calculations as well. In these popular methods there similarly are no lower bounds for the energies. The theoretical foundation of the four-component methods have been reviewed by Grant and Quiney [37], Kutzelnigg [103], Dyall [104] and Quiney et. al [20].

3.1.2 Restricted and unrestricted kinetic balance

Kinetically balanced basis set are characterized by the coupling between the large component, $\{\chi^L\}$, and small component, $\{\chi^S\}$, basis sets. The small component basis set must include the correct derivatives of the large component basis set,

$$\{\chi^S\} \supseteq \{\boldsymbol{\sigma} \cdot \boldsymbol{\nabla} \chi^L\}. \tag{3.2}$$

Quiney and Grant (e.g., [37, 53]) have argued that it is necessary to keep a strict one-to-one relationship between the basis functions. Each function in the small component basis must have a matching partner in the large component basis,

$$\chi_i^S = \boldsymbol{\sigma} \cdot \boldsymbol{\nabla} \chi_i^L, \tag{3.3}$$

for all basis functions. This gives a spectrum with an equal number of positive and negative energy solutions.

The discussion is first restricted to the single-particle central-field problem and two-spinor basis sets. The N basis functions $\chi_i^{L/S}$ are written as a radial function $\frac{1}{r} f_i^{L/S}$ times a normalized angular two-spinor (e.g., Eq. (2.25)). The kinetic balance relationship between the radial basis functions is then

$$f_i^S(r) = \left(\frac{d}{dr} + \frac{\kappa}{r} \right) f_i^L(r), \tag{3.4}$$

where κ is the quantum number defined in Sec. 2.2. For a particular angular shell with orbital angular quantum number l, a set of Gaussian basis functions with exponents $\{a\}$ for the large components are given by

$$f_a^L(r) = N_a^L r^{l+1} \exp(-ar^2). \tag{3.5}$$

The corresponding small component basis functions are

$$f_a^S(r) = N_a^S \left[(\kappa + l + 1) - 2ar^2 \right] r^l \exp(-ar^2), \tag{3.6}$$

where there is a fixed relationship between the two terms in the sum. Dyall and Fægri [105] termed the relationship given in Eq. (3.4) and (3.6) *restricted* kinetic balance

(RKB). One may show[2] that the overlap between two of these Gaussian two-spinors is given by

$$\langle \chi_a^L \mid \chi_b^L \rangle = \left(\frac{2\sqrt{ab}}{a+b} \right)^{l+3/2}, \tag{3.8}$$

$$\langle \chi_a^S \mid \chi_b^S \rangle = \left(\frac{2\sqrt{ab}}{a+b} \right)^{l+5/2}, \tag{3.9}$$

for the large and small components respectively. The small component overlap matrix is identical to the overlap matrix of a large component basis with the same set of exponents and angular quantum number $l+1$. Consequently the RKB prescription gives basis sets where the large and small component basis sets approach the basis set limit in a balanced fashion. The amount of linear dependence in the large and small component space will be approximately the same as the basis set dimensions are increased.

The relationship between the large and small components of the bound state four-spinor solutions, Eq. (2.22), may for a one-electron atom be written as

$$2mc\psi^S = -B(E)(\boldsymbol{\sigma} \cdot \boldsymbol{\nabla})\psi^L, \qquad B(E) = \left(1 + \frac{E-V}{2mc^2}\right)^{-1}. \tag{3.10}$$

The RKB operator $(\boldsymbol{\sigma} \cdot \boldsymbol{\nabla})$ therefore also gives the correct relationship between the large and small component one-particle *solutions* in the nonrelativistic limit ($c \to \infty$). Close to a heavy nucleus, however, $V(r)$ is in general not small compared to $2mc^2 = 37557.73$ a.u. For example, the zeroth order term in the series expansion of the potential from a Gaussian thallium nucleus is $V_0 = -1.08 \times 10^6$ a.u. (Paper II). Consequently the RKB operator does not correctly couple ψ^S and ψ^L in the important relativistic region close to the nucleus. It is simple to demonstrate that operation of the RKB operator on the exact large component radial function gives a function that is a very bad approximation to the exact small component function. On the basis of this it has been argued that RKB is 'wrong'. Since it is not possible to use potential and energy dependent basis sets as indicated by Eq. (3.10), one should keep as much flexibility as possible in the small component space and try to 'saturate' the small component basis set. This may be done by lifting the fixed relationship in Eq. (3.6), usually without increasing the computational cost significantly. Dyall and Fægri [105] used the term *unrestricted* kinetic balance (UKB) for basis sets where the number of small component basis functions is larger than the number of large component functions. The UKB prescription introduces extra variational parameters and gives a better description of the

[2]The overlap matrix elements are calculated by separating out the normalized angular part of the matrix element and by simple integration in the radial direction. The relationship

$$(\kappa + l + 1)(\kappa - l) = 0 \tag{3.7}$$

is useful in the calculation of the small component overlap matrix.

small component space, but will give rise to a number of extra negative energy solutions. There is no strict guarantee that they will lie below $-mc^2$. The extra 'unphysical' eigenvectors will have no contribution from the large components. They can have no kinetic energy since the kinetic energy is obtained from the coupling of the large and small components via the operator $(\boldsymbol{\sigma} \cdot \boldsymbol{p})$.

Both UKB and RKB have been used with success in molecular calculations. The intruder states that Grant and Quiney [37] warn against in UKB calculations have only been reported very rarely (e.g., [105]). It appears that a choice between the UKB and RKB scheme has not been of importance. The main reason is presumably that earlier investigations have been concerned with calculations of properties where the core region close to the nucleus mostly contributes as an effective potential. The name 'valence properties' will be used for properties of this type. In the work presented in Papers I and II, however, the quality of the molecular amplitudes close to a heavy nucleus is critically tested. In this region the RKB and UKB schemes are known to give different results [105].

3.1.3 Restricted kinetic balance by projection

The four-spinor single-particle solutions may be expanded in two-spinor basis functions. This is the method employed in the basis set version of GRASP [44, 45] that has been used for atomic calculations in this work. In DIRAC [21], however, the four-spinors are expanded in scalar basis functions, Eq. (2.48). Atomic centered Cartesian Gaussians,

$$G_{ijk}(\boldsymbol{r}, a) = N_{a,l} x^i y^j z^k \exp(-ar^2), \tag{3.11}$$

are used, where $i + j + k = l$ is the angular quantum number. $N_{a,l}$ is a normalization constant. For a given quantum number l, there are $\frac{1}{2}(l+2)(l+1)$ Cartesian Gaussians. This basis set may be transformed to a set of $2l + 1$ spherical Gaussians,

$$G_{lm}(\boldsymbol{r}, a) = N_{a,l} r^l \exp(-ar^2) Y_l^m(\theta, \phi), \tag{3.12}$$

where $Y_l^m(\theta, \phi)$ are spherical harmonics or real linear combinations of these. Given a large component basis set with angular quantum number l,

$$\{\chi^L\} = \{G_l(\boldsymbol{r}, a)\}, \tag{3.13}$$

the corresponding UKB small component basis set is best described as

$$\{\chi^S\} = \{G_{l-1}(\boldsymbol{r}, a), G_{l+1}(\boldsymbol{r}, a)\}. \tag{3.14}$$

This basis comprises all the Cartesian functions with $l - 1$ and $l + 1$. For $l = 0$ only $(l + 1)$-functions are non-zero. The usefulness of the dual family basis sets now becomes clear. The small component $l - 1$ partners for d- and f-type functions have already

been included in the basis set as the $l+1$ partners of the corresponding s- and p-type functions. The size of the small component basis set is significantly reduced with this choice of basis.

The strict RKB one-to-one relationship between large and small component basis functions is only possible in two-spinor basis. In Dyall's four-component program [16, 106] an RKB basis is generated in two steps. The first involves a radial contraction. Corresponding to a spherical large component basis set, $\{G_{lm}(\boldsymbol{r}, a)\}$, is the small component basis

$$\{\chi^S\} = \left\{ G_{l+1,m}(\boldsymbol{r}, a), \left(\frac{2ar^2}{2l+1} - 1 \right) G_{l-1,m}(\boldsymbol{r}, a) \right\}. \tag{3.15}$$

The RKB one-to-one relationship is then obtained after an angular transformation[3]. This relationship may also be obtained by another procedure suggested by Saue [107]. This scheme for RKB by projection is summarized below.

The Dirac–Hartree–Fock equations on matrix form are given by (e.g., [21])

$$\mathbf{FC} = \mathbf{eSC}. \tag{3.18}$$

The solution procedure involves a transformation to an orthonormal basis

$$\mathbf{\Phi} = \chi \mathbf{U}, \tag{3.19}$$

and a subsequent diagonalization of the Fock matrix, $\mathbf{F}$, in this basis. In DIRAC [21] the canonical orthonormalization procedure [108], Löwdin orthonormalization, may be used to generate the transformation matrix, $\mathbf{U}$. The advantage of this method is that linear dependence in the basis set may be projected out in the transformation from atomic centered basis functions (AO-basis) to orthonormal four-spinors (MO-basis).

An RKB calculation with spherical large component basis, is performed in DIRAC by the following procedure:

[3] An example will illustrate the angular transformation. A large component s-function coupling with spin gives the two $\kappa = -1$ two-component spinors in Table 2.1,

$$\begin{pmatrix} s \\ 0 \end{pmatrix}, \quad \begin{pmatrix} 0 \\ s \end{pmatrix}. \tag{3.16}$$

The corresponding small component two-spinors are

$$\begin{pmatrix} -p_0 \\ \sqrt{2}p_1 \end{pmatrix}, \quad \begin{pmatrix} -\sqrt{2}p_{-1} \\ p_0 \end{pmatrix}, \tag{3.17}$$

where $p_0 = p_z$, $p_1 = p_x + ip_y$ and $p_{-1} = p_x - ip_y$. However, the coupling of the small component functions p_x, p_y and p_z with spin gives six linearly independent two-spinors. Two linear combinations are the ones given in Eq. (3.17), but the four others have no large component partner in the s-spinor set. If they are not removed these 'orphan' small component functions will give rise to four extra 'unphysical' negative energy solutions in the spectrum. These solutions have zero large components and consequently no kinetic energy.

1. The large component overlap matrix is transformed to spherical basis and the small component matrix to a radially contracted scalar basis, Eq. (3.15). The canonical orthonormalization matrix in spherical or radially contracted basis is generated,

$$\mathbf{V} = \mathbf{O}\mathbf{s}^{1/2}, \tag{3.20}$$

   where $\mathbf{O}$ is the matrix that diagonalizes the overlap matrix, $\mathbf{S}$, in Eq. (3.18). In accordance with the Löwdin orthonormalization procedure [108], linear dependence is removed. Eigenvectors corresponding to eigenvalues, s_i, below a certain threshold are deleted in $\mathbf{V}$. Thresholds of 10^{-6} and 10^{-8} are used for the large and small components respectively. Finally the rows of $\mathbf{V}$ are backtransformed to Cartesian basis. The rectangular transformation matrix $\mathbf{U}'$ is obtained. It projects out the undesired parts of the Cartesian basis set.

2. The free-particle Dirac–Hartree–Fock equation, that is Eq. (3.18) where $\mathbf{F}$ is the free-particle Fock matrix, is solved. $\mathbf{U}'$ is used in the orthogonalization procedure.

3. All the coefficients corresponding to 'unphysical' negative energy solutions are removed from the set of MO-coefficient obtained from the free-particle calculation. They are easily found since they have zero kinetic energy and only rest energy in the free-particle system. The remaing MO-coefficient matrix is used as MO-transformation matrix, $\mathbf{U}$, in the subsequent Dirac–Hartree–Fock iterations.

This MO-transformation now projects out all components of the basis set that do not correspond to a spherical large component basis and a small component basis generated by the RKB prescription. The same number of positive and negative energy solutions are obtained in the single-particle spectrum. The scheme is simple and has large flexibility. Cartesian and spherical large component basis sets with UKB small component basis can be obtained by omitting steps in the procedure above.

The above RKB scheme has been developed and implemented in DIRAC by T. Saue. The radial contraction has been implemented by the author. The contraction removes the most serious linear dependence in the basis set. Together, the projection scheme and radial contraction gives a simple method for generating basis sets in accordance with the RKB prescription from scalar basis sets. The method is numerically stable and removes the linear dependence that causes serious problems in the UKB scheme. This will be demonstrated in the next section. A separate paper on the RKB projection scheme and its applications is in preparation [107].

3.2 Basis set experiments

3.2.1 Energy-optimized basis sets

The first relativistic basis set optimization program [109] has only recently been developed. Common practice in relativistic four-component calculations has been to use energy-optimized basis sets from a nonrelativistic basis set optimization. Basis sets of this type are known to give a good description also of the relativistic system, as long as extra p-functions are added to describe the core region of the $\kappa = +1$ spinors. A 22s17p13d8p thallium dual family basis set has been optimized in the nonrelativistic program TANGO [110] with a point nucleus. In a stepwise procedure, two additional high-exponent p-functions were optimized in GRASP, and the basis set was augmented with these two functions. The final dual family 22s19p13d8p basis set is given in Table 3.1. The main characteristics of an energy-optimized basis set for a heavy element can be seen from this table. There are high exponent functions of the order 10^7 for the s-functions and 10^6 for the p-functions, but there is a much lower 'density' of basis functions in the core region compared with the intermediate subvalence region. In the valence region the density is again lower. Basis sets used in molecular calculations are usually augmented with extra diffuse functions for all angular quantum numbers in order to describe the molecular systems better and get reasonable virtual orbitals for correlated calculations.

The thallium basis set in Table 3.1 is of reasonably high quality, for example for the calculation of energies or valence properties such as bond lengths and vibrational frequencies. However, in the introduction to this chapter it was mentioned that in the nuclear region the wavefunction is Gaussian in shape with exponent 1.066×10^7 for the large component of a $\kappa = -1$ spinor. The exponent for the small component of a $\kappa = +1$ spinor is of the same order of magnitude. It is of course not possible to model such a function with exponents lower than this value. One would also assume that in order to get a reasonable description, a sufficiently high density of functions in the core region is necessary. The $(p_0/q_0)^\kappa$-value is a critical test of to the quality of the wavefunction in the nuclear region. It has been calculated for hydrogen-like thallium, and the results (RKB calculation) are given in Table 3.1. For comparison finite difference calculations have been performed with GRASP [44]. These results are regarded as being the Dirac–Hartree–Fock limit, and they are given in Table 3.4 and 3.6. The basis set in Table 3.1 gives values that are in error by approximately 5% for $\kappa = -1$ and too low by a factor 2.7 for $\kappa = +1$.

A similar test of a relativistic energy-optimized thallium basis set is described in Paper II. The results for the $(p_0/q_0)^\kappa$-values are of the same poor quality as for the nonrelativistic basis set described above, especially for the $\kappa = +1$ spinors. The analysis shows that without significant improvements in the nuclear region, energy-optimized basis sets can not be used for calculations of properties where the correct structure of the wavefunction

Table 3.1: Energy-optimized 22s19p13d8p thallium dual family basis set. Two extra high-exponent basis function have been added in the p-set in order to describe the $p_{1/2}$-spinors. The ratio between each exponent and the preceeding exponent $(\lambda_i/\lambda_{i-1})$ is given, in addition to the $(p_0/q_0)^\kappa$-values from a Gaussian nucleus calculation on relativistic hydrogen-like thallium, Tl^{80+}.

s (d) basis set exponents		$(\lambda_i/\lambda_{i-1})$	p (f) basis set exponents		$(\lambda_i/\lambda_{i-1})$	
44866069.253429			3080000.000000			One-electron
6716872.914589		6.7	445000.000000		6.9	system,
1529759.805675		4.4	67089.131245		6.6	$(p_0/q_0)^\kappa$:
433540.390987		3.5	15891.451181		4.2	$1s_{1/2}$: -2753.24
141449.368601		3.1	5155.394335		3.1	$2s_{1/2}$: -2759.55
50990.841049		2.8	1963.817613		2.6	$3s_{1/2}$: -2760.59
19757.098234		2.6	825.381167		2.4	$2p_{1/2}$: 1007.94
8041.509265		2.5	369.383849	(f)	2.2	$3p_{1/2}$: 1009.09
3382.647083	(d)	2.4	172.854978	(f)	2.1	
1466.494604	(d)	2.3	83.350095	(f)	2.1	
655.480315	(d)	2.2	40.242273	(f)	2.1	
293.244986	(d)	2.2	19.623221	(f)	2.1	
139.110039	(d)	2.1	9.500754	(f)	2.1	
67.808539	(d)	2.1	4.515324	(f)	2.1	
33.794148	(d)	2.0	1.903470	(f)	2.1	
16.738579	(d)	2.0	.834782		2.3	
8.159197	(d)	2.0	.330628		2.5	
3.936294	(d)	2.1	.113565		2.9	
1.727149	(d)	2.3	.039247		2.9	
.718297	(d)	2.4				
.267865	(d)	2.7				
.076573		3.5				

close to the nucleus is of importance.

3.2.2 Even-tempered basis sets

Even-tempered basis sets, Eq. (3.1), were used in basis set experiments to investigate the convergence of $(p_0/q_0)^\kappa$-values and energy eigenvalues with basis set size. The basis sets are defined in Table 3.2. Calculations were performed on hydrogen-like thallium with a Gaussian nucleus. In order to cover a sufficient range of exponents, the highest exponent in the basis set was chosen to be 5.0×10^8 for all the sets. The lowest exponent was 0.04, and the different basis sets are characterized by different densities of exponents given by the parameter β. The small component basis sets were generated by RKB (the projection method in Sec. 3.1.3) for the test calculations on the $\kappa = -1$ and $\kappa = +1$ one-electron systems. In the UKB sets all the small component functions that are generated from the coupling of the scalar small component basis with spin have been kept. Note that RKB and UKB give identical bound state solutions for $\kappa = -1$ since the extra 'orphan' basis functions do not couple with the other functions in the set. For $\kappa = +1$ there is a larger number of functions in the small component UKB basis set, and this may give a better description of the small component compared with RKB. The smallest eigenvalue of the overlap matrices are also given in the Table 3.2. A small value for the lowest eigenvalue of the overlap matrix is an indication of linear dependence in the basis set. Calculations on spinors where $|\kappa| > 1$ were not performed since these spinors have zero amplitudes at the nucleus.

The results for the $\kappa = -1$ spinors $1s_{1/2}$, $2s_{1/2}$ and $3s_{1/2}$ are given in Table 3.3 and 3.4. The energies converge smoothly (from above) towards the finite difference results from GRASP [44], and the largest basis set is only 7×10^{-8} a.u. above the finite difference result. All the basis sets are without serious linear dependence in both the large and small component space. This is seen from Table 3.2 where the smallest eigenvalue of the overlap matrix is larger that 10^{-6} for all the basis sets. Table 3.4 shows the convergence of the more demanding $(p_0/q_0)^\kappa$-value. A plot of the $(p_0/q_0)^\kappa$-values for the $1s_{1/2}$-spinor is given in Figure 2 of Paper II. These numbers are also converging with basis set size, but much slower than the energy eigenvalues. Reasonable results are obtained for all the basis sets better than b4, but there are quite large errors for all the basis sets except b8, b9 and b10. There is also slower convergence for higher principal quantum number n. This is expected, since a high value for n corresponds to a large number of 'wiggles' and a lower density in the nuclear region.

Results for the $\kappa = +1$ spinors $2p_{1/2}$ and $3p_{1/2}$ are given in Table 3.5 and 3.6. The UKB and RKB results are not identical, but both converge smoothly with basis set size towards the finite difference results both for the energy eigenvalue and $(p_0/q_0)^\kappa$. In analogy with $\kappa = -1$ the $(p_0/q_0)^\kappa$-values converge more slowly than the energy eigenvalues. The RKB $(p_0/q_0)^\kappa$-values of the $2p_{1/2}$-spinor are plotted in Figure 3 of Paper II. However, the dramatic difference between UKB and RKB is seen from the smallest

Table 3.2: Parameters for even-tempered basis sets of N functions where the exponents are defined by the prescription in Eq. 3.1. The exponents are in the range from $\lambda_1 = 0.04$ to $\lambda_N = 5.0 \times 10^8$ for all the basis sets (Identical to the ten last basis sets in Table I, Paper II). The parameter β is given in the table together with the smallest eigenvalue, $s_{\pm 1}$, of the large (L) and small (S) component overlap matrix for $\kappa = \pm 1$ systems. The small component results for $\kappa = +1$ are given both for restricted (RKB) and unrestricted kinetic balance (UKB). The smallest eigenvalue of the $\kappa = +1$ large component and $\kappa = -1$ small component overlap matrices are identical (Sec. 3.1.2).

Basis	N	β	s_{-1} (L)	s_{+1} (L) and s_{-1} (S)	s_{+1} (S,RKB)	s_{+1} (S,UKB)
b1	21	3.026	8.812×10^{-3}	3.309×10^{-2}	7.829×10^{-2}	7.147×10^{-5}
b2	23	2.748	4.334×10^{-3}	1.781×10^{-2}	4.574×10^{-2}	1.801×10^{-5}
b3	25	2.534	2.107×10^{-3}	9.403×10^{-3}	2.608×10^{-2}	4.434×10^{-6}
b4	27	2.366	1.014×10^{-3}	4.886×10^{-3}	1.456×10^{-2}	1.062×10^{-6}
b5	29	2.229	4.842×10^{-4}	2.504×10^{-3}	7.981×10^{-3}	2.501×10^{-7}
b6	31	2.117	2.294×10^{-4}	1.268×10^{-3}	4.306×10^{-3}	5.791×10^{-7}
b7	33	2.023	1.080×10^{-4}	6.355×10^{-4}	2.291×10^{-3}	1.321×10^{-7}
b8	35	1.943	5.057×10^{-5}	3.155×10^{-4}	1.204×10^{-3}	2.976×10^{-9}
b9	37	1.875	2.356×10^{-5}	1.554×10^{-4}	6.254×10^{-4}	6.625×10^{-10}
b10	39	1.815	1.092×10^{-5}	7.595×10^{-5}	3.217×10^{-4}	1.460×10^{-10}

Table 3.3: Basis set convergence of the $1s_{1/2}$, $2s_{1/2}$ and $3s_{1/2}$ energy eigenvalue of hydrogen-like thallium, Tl^{80+}. The even-tempered basis sets are defined in Table 3.2. The restricted kinetic balance and unrestricted kinetic balance results are identical, and they are compared with the finite difference results (FD).

Basis	$1s_{1/2}$	$2s_{1/2}$	$3s_{1/2}$
b1	-3629.33754083	-930.29016487	-401.09335761
b2	-3629.42505217	-930.49035020	-402.77989149
b3	-3629.44261926	-930.59397552	-402.86955851
b4	-3629.44605508	-930.60726924	-402.93087822
b5	-3629.44687020	-930.61012660	-402.98202254
b6	-3629.44708519	-930.61188801	-402.98251407
b7	-3629.44713487	-930.61218712	-402.98627903
b8	-3629.44714440	-930.61223241	-402.98694392
b9	-3629.44714621	-930.61225691	-402.98704778
b10	-3629.44714663	-930.61226134	-402.98713273
FD	-3629.44714670	-930.61226239	-402.98714291

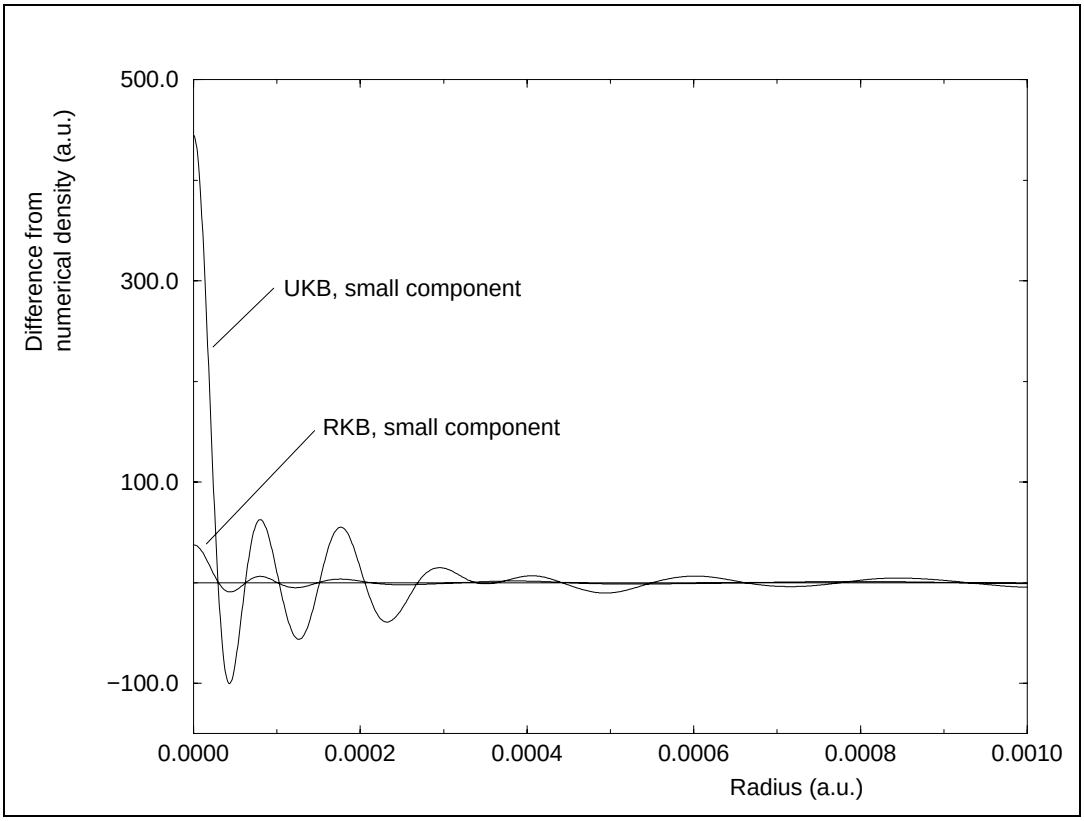

Figure 3.1: The difference between the finite basis set (basis b7, Table 3.2) and finite difference radial wavefunction for the small component of the $2p_{1/2}$-spinor of Tl^{80+}. Both the restricted (RKB) and unrestricted kinetic balance (UKB) results are shown. At this scale the RKB and UKB large component wavefunctions are identical. The root-mean-square radius of the atomic nucleus is 1.0392×10^{-4} a.u.

Table 3.4: Basis set convergence of the $1s_{1/2}$, $2s_{1/2}$ and $3s_{1/2}$ $(p_0/q_0)^\kappa$-value of hydrogen-like thallium, Tl^{80+}. The even-tempered basis sets are defined in Table 3.2. The restricted kinetic balance and unrestricted kinetic balance results are identical, and they are compared with the finite difference results (FD).

Basis	$1s_{1/2}$	$2s_{1/2}$	$3s_{1/2}$
b1	-2594.07	-2618.53	-2766.85
b2	-2637.02	-2599.12	-2528.38
b3	-2623.09	-2656.40	-2629.64
b4	-2626.38	-2628.16	-2675.07
b5	-2621.63	-2623.75	-2613.13
b6	-2617.14	-2627.58	-2618.34
b7	-2615.18	-2620.69	-2630.33
b8	-2612.89	-2619.09	-2620.31
b9	-2611.89	-2618.88	-2617.74
b10	-2611.31	-2617.77	-2619.91
FD	-2611.28	-2617.84	-2619.12

eigenvalue of the overlap matrices in Table 3.2. The value for the small component UKB basis is three to six orders of magnitude smaller than the corresponding value for RKB, and there is severe linear dependence in the largest basis sets. This does not seem to influence the one-electron parameters in Table 3.5 and 3.6 which are calculated simply by diagonalizing the one-electron Fock matrix. However, the linear dependence must be removed in many-electron calculations to avoid calculations that do not converge, meaningless correlated energies and so on. Linear dependence has been removed in three of the basis sets by Löwdin orthonormalization (eigenvectors of the small component overlap matrix with eigenvalues below 10^{-8} have been projected out). The results are given in the footnotes of Table 3.5 and 3.6. In summary, both the UKB and RKB results converge smoothly with basis set size towards the finite difference result, but UKB gives less accurate results when linear dependence has been removed. It does not appear that the UKB $(p_0/q_0)^\kappa$-value will converge with basis set size (Table 3.6). Another demonstration of the linear dependence problems in the UKB basis sets is provided by Figure 3.1. In the figure the difference between the finite difference and basis set (b7) small component radial amplitudes for both RKB and UKB are given. The large oscillations or 'wiggles' for the UKB wavefunction clearly illustrates the lower quality of this approach. Dyall and Fægri [105] have earlier obtained similar results.

Table 3.7 and 3.8 show the effect of adding a single additional even-tempered function to the basis set b7 (b7+1) and of removing the n (b7-n, n= 1, 2, 3, 4) innermost functions. All the results are from RKB calculations. The basis sets b7-3 and b7-4 have large errors for $(p_0/q_0)^\kappa$, demonstrating that this parameter is only calculated correctly with basis

Table 3.5: Basis set convergence of the $2p_{1/2}$ and $3p_{1/2}$ energy eigenvalue of hydrogen-like thallium, Tl^{80+}, for the basis sets defined in Table 3.2. The restricted kinetic balance (RKB) and unrestricted kinetic balance (UKB) results are given in the table. There is severe linear dependence in the UKB basis sets b8, b9 and b10. The energies for the system after removal of linear dependence by Löwdin orthonormalization, are given in the footnotes.

Basis	$2p_{1/2}$ (RKB)	$2p_{1/2}$ (UKB)	$3p_{1/2}$ (RKB)	$3p_{1/2}$ (UKB)
b1	-930.79269012	-930.79131611	-402.34607526	-402.34536742
b2	-930.90155693	-930.90122876	-402.68696226	-402.68676512
b3	-930.94383669	-930.94375904	-403.03758729	-403.03754395
b4	-930.95895856	-930.95894075	-403.05646319	-403.05645190
b5	-930.96162423	-930.96162005	-403.08138999	-403.08138709
b6	-930.96231143	-930.96231031	-403.08890342	-403.08890283
b7	-930.96255626	-930.96255584	-403.08971150	-403.08971133
b8	-930.96260173	-930.96260147[1]	-403.09049061	-403.09049057[2]
b9	-930.96261185	-930.96261163[1]	-403.09057322	-403.09057322[2]
b10	-930.96261517	-930.96261497[1]	-403.09061374	-403.09061374[2]
FD	-930.96261577		-403.09062751	

[1] The eigenvalues calculated after removal of the severe linear dependence in basis sets b8, b9 and b10 are given by

b8	-930.96260447
b9	-930.96261271
b10	-930.96261526

[2] The eigenvalues calculated after removal of the severe linear dependence in basis sets b8, b9 and b10 are given by

b8	-403.09049211
b9	-403.09057452
b10	-403.09061432

Table 3.6: Basis set convergence of the $2p_{1/2}$ and $3p_{1/2}$ $(p_0/q_0)^\kappa$-value of hydrogen-like thallium, Tl^{80+}, for the basis sets defined in Table 3.2. The restricted kinetic balance (RKB) and unrestricted kinetic balance (UKB) results are given in the table. There is severe linear dependence in the UKB basis sets b8, b9 and b10. The calculated values after removal of linear dependence by Löwdin orthonormalization, are given in the footnotes.

Basis	$2p_{1/2}$ (RKB)	$2p_{1/2}$ (UKB)	$3p_{1/2}$ (RKB)	$3p_{1/2}$ (UKB)
b1	2696.88	2663.04	2698.76	2664.54
b2	2709.24	2686.73	2706.45	2688.10
b3	2713.55	2698.37	2716.81	2699.70
b4	2713.20	2704.03	2715.32	2705.34
b5	2713.08	2706.74	2713.13	2708.05
b6	2711.99	2708.03	2713.54	2709.31
b7	2710.81	2708.64	2712.38	2709.92
b8	2710.11	2708.93[1]	2711.25	2710.20[1]
b9	2709.60	2709.07[1]	2710.87	2710.40[2]
b10	2709.28	2709.14[1]	2710.65	2710.44[2]
FD	2709.20		2710.48	

[1] $(p_0/q_0)^\kappa$ calculated after removal of the severe linear dependence in basis sets b8, b9 and b10 are given by

b8	2713.71
b9	2707.03
b10	2710.37

[2] $(p_0/q_0)^\kappa$ calculated after removal of the severe linear dependence in basis sets b8, b9 and b10 are given by

b8	2716.67
b9	2703.72
b10	2714.17

Table 3.7: Basis set experiments on the $1s_{1/2}$-state of hydrogen-like thallium, Tl^{80+}. Restricted kinetic balance results for the even-tempered basis set b7 (Table 3.2) are compared with finite difference results (FD) and basis sets derived from b7. The basis set b7+1 was constructed from b7 by adding one extra high exponent function in the even-tempered series. In b7-n, n=1,2,3,4, the n inner basis functions were removed from b7.

Basis	Energy	$\langle 1/r \rangle$	$\langle 1/(r^2) \rangle$	$\langle r^2 \rangle$	$(p_0/q_0)^\kappa$
b7-4	-3629.43538538	100.2239717	25138.79018	3.602402228×10^{-4}	-2221.49
b7-3	-3629.44671360	100.2259731	25178.59728	3.602379115×10^{-4}	-2525.04
b7-2	-3629.44713545	100.2261488	25186.52770	3.602378220×10^{-4}	-2614.22
b7-1	-3629.44713487	100.2261514	25186.78102	3.602378222×10^{-4}	-2607.64
b7	-3629.44713486	100.2261515	25186.78852	3.602378222×10^{-4}	-2615.18
b7+1	-3629.44713487	100.2261514	25186.78167	3.602378222×10^{-4}	-2606.10
FD	-3629.44714670	100.2261518	25186.78426	3.602377871×10^{-4}	-2611.28

Table 3.8: Basis set experiments on the $2p_{1/2}$ state of hydrogen-like thallium, Tl^{80+}. Restricted kinetic balance results for the even-tempered basis set b7 (Table 3.2) are compared with finite difference results (FD) and basis sets derived from b7. The basis set b7+1 was constructed from b7 by adding one extra high exponent function in the even-tempered series. In b7-n, n=1,2,3,4, the n inner basis functions were removed from b7.

Basis	Energy	$\langle 1/r \rangle$	$\langle 1/(r^2) \rangle$	$\langle r^2 \rangle$	$(p_0/q_0)^\kappa$
b7-4	-930.96244389	26.41058818	1312.635951	3.307529286×10^{-3}	2347.95
b7-3	-930.96255315	26.41061312	1313.087441	3.307528245×10^{-3}	2629.63
b7-2	-930.96255625	26.41061475	1313.161309	3.307528210×10^{-3}	2710.11
b7-1	-930.96255625	26.41061473	1313.159957	3.307528210×10^{-3}	2707.25
b7	-930.96255626	26.41061474	1313.161366	3.307528210×10^{-3}	2710.80
b7+1	-930.96255626	26.41061474	1313.160396	3.307528210×10^{-3}	2707.65
FD	-930.96261577	26.41061780	1313.160821	3.307523401×10^{-3}	2709.20

sets where exponents at least as high as 1.5×10^8 are included. Adding extra functions with higher exponents beyond this value does not seem to improve the ability of the basis set to give correct $(p_0/q_0)^\kappa$-ratios for the system. The calculated value continues to 'oscillate' around the finite difference result. Smaller oscillations have been observed in other experiments with basis sets with smaller β-values. The energy eigenvalues and expectation values of r^n $(n = -2, -1, 2)$ have also been calculated. All these properties converge much faster with basis set size than $(p_0/q_0)^\kappa$. This again provides an illustration of the difficulties with this single-point parameter compared with the much less demanding 'average' properties.

Calculations have also been performed for many-electron systems (Xe, Rn and neon-like thallium). For these Dirac–Hartree–Fock calculations (which also provide single-particle type solutions), the convergence of $(p_0/q_0)^\kappa$ with basis set is neither better nor worse than in the one-electron systems. It has also been demonstrated that two-spinor RKB (GRASP [44, 45]) and RKB by projection as described in Sec. 3.1.3, give results that are identical to numerical accuracy for these systems.

3.3 Conclusions

From the results above one may conclude that the warnings of Grant and Quiney regarding the convergence of the basis sets towards the basis set limit are highly relevant. Any reasonable uncontracted basis set that may be used for molecular or atomic calculations will have more than sufficient flexibility in the RKB small component space to describe the correct relationship between the large and small component solutions, Eq. (3.10). The extra flexibility in the UKB basis set is not necessary and may give rise to severe linear dependence and oscillations in the amplitudes close to the nucleus as seen in Figure 3.1. Attempts on projecting out the linear dependence have given less accurate results than RKB. However, UKB has not given completely wrong results in any of the experiments that have been performed. In calculations of valence properties, where the core region only enter as an effective potential, it is not expected that a choice between RKB and UKB will be of importance.

Even-tempered basis sets give values for $(p_0/q_0)^\kappa$ that converge towards the Dirac–Hartree–Fock limit when the parameter defining the 'density' of the basis set, β, is reduced. However, it is necessary to have basis functions with sufficiently high exponents and a high density of exponents all the way in to the nuclear region both in the s- and p-function set.

The experiments described in the previous sections and other similar experiments have provided the author with some experience about basis set requirements:

- With a finite nuclear model one is modelling Gaussian shaped spinors with exponents of the order 1×10^7 in the nuclear region. Both the large component $\kappa = -1$

and the small component $\kappa = -1$ spinors are of this type. It appears that in practical calculations the largest s- and p-type basis functions should be at least 4×10^8 and 2×10^8 respectively.

- A high density of functions is needed all the way in to the nuclear region. The β-value must not be significantly higher than 2.2 anywhere in the basis set. One may use energy-optimized basis sets if the core-region basis functions are replaced by a series of even-tempered functions with sufficiently low β. However, the advantage of using even-tempered basis sets is that one may test the convergence of the calculated property simply by varying the single parameter β.

- In the intermediate and valence regions the s-, p-, d- and f-type basis sets must at least correspond to ordinary 'valence property' basis sets. Lower quality gives inaccurate results for the amplitudes in the nuclear region.

- Restricted kinetic balance gives a balanced convergence of the basis set with respect to basis set size. UKB gives severe linear dependence in the small component space.

Following these simple rules, one should obtain correct amplitudes in the neighbourhood of a heavy nucleus in molecular basis set calculations.

Chapter 4

Summary of papers

4.1 PT-odd interactions in TlF studied by the Dirac–Hartree–Fock method

Papers I and II of this thesis describe Dirac–Hartree–Fock calculations of the electronic structure of thallium fluoride. We are concerned with the interpretation of nuclear magnetic resonance experiments on molecular beams of thallium fluoride. In these experiments the hyperfine structure of the molecule has been studied in the presence of external parallel magnetic and electric fields. A non-zero frequency shift upon reversal of one of the external fields would be the signature of an electric dipole moment (edm) parallel to a magnetic moment and a demonstration of a process in nature that is not symmetric with respect to space and time inversion (PT-odd). It is remarkable that these and similar atomic and molecular beam low energy experiments may give important contributions to high energy elementary particle physics within and in the case of edm's beyond the 'standard model' of electroweak interactions. The T-odd decay of the K^0 meson is still not fully understood. The current null-results from the thallium fluoride experiments may be used to place restrictions on physical theories that have been proposed in order to explain the T-odd process and which go beyond the electroweak model. However, to relate the experimental data to fundamental constants it is necessary to perform accurate electronic structure calculations. It is with these calculations we are concerned in Papers I and II. Earlier work on this problem has been performed with nonrelativistic methods and quite small basis sets, and relativistic effects have been introduced by fitting the nonrelativistic amplitudes to amplitudes from relativistic atomic calculations [111, 112]. These previous studies can at best provide order of magnitude estimates for the parameters involved in the interpretation of the experiments.

The fully relativistic Dirac–Hartree–Fock calculations presented in Papers I and II are

one of the first investigations where the quality of the molecular four-component wavefunction is critically tested in the region of a heavy atomic nucleus. In this region the relativistic effects are *very important*. This can be seen by comparing the relativistic and nonrelativistic values of the PT-odd parameter X which is proportional to the gradient of the electron density at the center of the thallium nucleus. Their values differ by more than a factor seven. Earlier studies of the molecular four-component wavefunction have focused on average properties such as energy eigenvalues of core orbitals, total energies and various expectation values. The important PT-odd parameter X depends on the amplitudes at a single point and has contibutions of the same order of magnitude from the large and small components. It is not know to the author that properties of this type have been studied previously by four-component methods. In our study we demonstrate that high accuracy for the average properties provide insufficiently rigorous tests of basis set quality in the calculation of X. Instead, our analysis in Paper II shows that a suitable test for the basis sets is provided by the ratio p_0/q_0 from atomic calulations. This is the ratio of the leading terms in the power series expansion of the large and small component amplitudes. In has been shown that calculations of the p_0/q_0-ratio and the PT-odd parameters requires large uncontracted basis sets with a high density of basis functions in the high exponent nuclear region.

In order to check the quality of our calculated parameters extensive tests were performed. In addition to the tests of convergence with basis set size described above, the influence of basis set superposition error (BSSE) was tested by introducing ghost nuclei in the molecular calculations and in atomic calculations of the PT-odd parameters. It was also demonstrated that the nonvanishing electric field at the thallium nucleus at the equilibrium bond length was caused mainly by the low flexibility of the f-shell. When extra g-type polarization functions were added in the basis set reasonable agreement with the Hellmann–Feynman theorem was obtained. Both BSSE effects and the low flexibility of the f-shell were demonstrated to have very little influence on the total values for the PT-odd parameters. The various core-spinor values were significantly influenced, but this gave a negligible contribution to the total values due to the orthonormality constraints of the molecular orbitals.

The very large basis sets that were necessary in the calculations gave severe linear dependence problems when unrestricted kinetic balance was employed. This is to our knowledge the first study where the use of restricted kinetic balance has been of importance for the quality of the result. Our findings will be of relevance in future studies of properties where the quality of the amplitudes in the nuclear region of a heavy atom is significant.

Careful analysis and elimination of errors in the Dirac–Hartree–Fock calculations enable us to place new bounds on PT-odd effects in thallium fluoride using existing experimental data. Together with our theoretical parameters these data are now placing the most restrictive available bounds on the electric dipole moment of the proton, the Schiff-moment of the thallium nucleus due to PT-odd nuclear interactions and the PT-odd

tensor coupling constant. In Paper II we review the theory of PT-odd effects in thallium fluoride.

The molecular and atomic calculations presented in Papers I and II have been performed by the author of this thesis. The analysis and interpretation of the results were done in cooperation with H.M. Quiney.

4.2 Direct four-component MP2 and application to coinage metal fluorides

The relativistic Dirac–Hartree–Fock method is a single-particle model, and in analogy with the nonrelativistic Hartree–Fock method it provides solutions of limited quality for most systems. Electron correlation has to be included to obtain quantitative results for most chemical properties. The implementation of direct four-component Møller-Plesset perturbation theory to second order (MP2) is described in Paper III. The MP2 method recovers the major part of the correlation energy for most closed-shell systems and at a lower cost than for all other correlated methods. In the direct MP2 method the integrals are recalculated as they are needed, and I/O and external memory bottlenecks are avoided. These recalculations, however, are not very expensive. For computers with sufficiently large internal memory the number of floating point operations is only doubled compared with a conventional disk based scheme.

The scalar basis sets employed in four-component calculations are more than twice the size of the basis sets for the corresponding nonrelativistic calculations. However, the active molecular orbital spaces employed in correlated calcualtions are of approximately the same size since in the relativistic case all the negative energy solutions are neglected within the no-pair approximation. Systems where relativistic effects are of importance also have a large number of core electrons. It is not necessary to correlate these in calculations of valence properties. This means that when the Dirac–Hartree–Fock calculation has been performed and the integrals have been transformed to molecular basis, the actual calculation of the correlation energy is cheap. In relativistic calculations it is therefore usually the four-index transformation of the two-electron integrals that is the most demanding step. The MP2 method is extreme in this sense. In an average calculation where the CPU time for one Dirac–Hartree–Fock iteration is 30 minutes, the four-index transformation takes a few CPU hours and the actual calculation of the energy takes perhaps 10 CPU seconds. The greatest advantage of the MP2 method is that the energy is calculated from two-electron integrals of the type (ov|ov) where o is an occupied and v is a virtual orbital. In all other correlated methods the much larger class of (vv|vv)-integrals is also needed. This class of integrals is more than an order of magnitude larger than the (ov|ov)-class in the average case.

Correlated calculations are most efficient if there is a balance between the basis set

quality and the accuracy of the method [113], and accurate correlated methods are only useful if they can be employed with large and flexible basis sets. The rather inexpensive MP2 method is therefore useful since one may experiment with large basis sets and active spaces without running into prohibitively expensive calculations.

The MP2 method has been applied in calculations on CuF, AgF and AuF. It is especially for AuF that relativistic effects are important, and significant non-additivity of relativistic and correlation effects were found. This is the case for most molecules that have been studied in correlated four-component calculations, and it is now well established that correlation and relativistic effects can not simply be added since the cross terms may be quite significant. Schwerdtfeger et al. [114] have studied the relativistic contraction in a series of diatomic gold compounds with pseudopotential methods at the SCF level. They find an almost linear relationship between the relativistic contraction of the bond and the electronegativity of the ligand. This relationship appears to persist if one compares our four-component SCF calculations for AuF with the very similar calculations of Collins et al. [115] for AuH. However, at the MP2 level there is almost no difference between the relativistic contractions of AuF and AuH. It is too early to draw any conclusions from only two molecules, but it appears that one should be very careful with conclusions based purely on SCF calculations. It is interesting to note that *most* 'well-known' relativistic effects have been established from only molecular or atomic mean-field calculations. For this reason the correlated methods are extremely useful for the verification of earlier less accurate studies.

The development of the algorithm, the implementation of the direct MP2 method and the calculations in Paper III have been performed by the author of this thesis. The direct algorithm is partially based on the nonrelativistic direct MP2 scheme of Head-Gordon et al. [116].

4.3 Four-component MP2 study of the lanthanide and actinide contraction

The direct MP2 program presented in Paper III has been integrated in the DIRAC program system [21]. In connection with this work a new version of the four-index transformation has been implemented. Point group symmetry is used in a quaternion formalism to reduce significantly the cost of the calculations. With this new version of the MP2 program, the MP2 calculation always costs less than the full Dirac–Hartree–Fock calculation.

The new version of the MP2 program has been used in the fully relativistic study of the lanthanide and actinide contraction that is presented in Paper IV. This is one of the first correlated four-component studies where trends have been followed both horizontally and vertically in the periodic system and where a number of molecules

have been studied. In this respect it represents a progress compared with most earlier four-component studies of heavy-element molecules.

The chemical results presented in Paper IV are of importance for the structural chemistry of heavy elements. In at least a decade it has been 'well-known' that '... the lanthanide contraction is also partly due to relativistic effects...' [117]. This knowledge has mainly been based on atomic and molecular mean-field calculations [6, 9]. It is, however, not obvious that this is generally correct, and recent high quality correlated pseudopotential calculations [118] give a relativistic *decrease* of the lanthanide contraction for the lanthanide hydrides. In Paper IV it is demonstrated that for the three types of molecules that have been studied between, 10% and 30% of the lanthanide contraction is a relativistic effect. This result is obtained provided that sufficiently large active spaces are used in the correlated calculations. In this study we have therefore been able to gauge the important *increase* of the lanthanide contraction due to relativity in fully relativistic correlated calculations. For the actinides as much as 50% of the contraction is caused by relativity, and the larger size of the actinide compared with the lanthanide contraction is a relativistic effect.

It has often been claimed that four-component methods are very useful for benchmark calculations in order to test more approximate methods. There are many Dirac–Hartree–Fock programs available, but with a few exceptions (e.g., [115, 119]) there appears to be few cases where these codes actually have been used to test other relativistic approaches. The work in Paper IV employs basis sets of similar quality to the valence basis sets of an earlier pseudopotential study on the lanthanide and actinide contraction by Küchle et al. [118]. By comparing our results with the high quality correlated results of [118] we were able to establish the accuracy of the MP2 method for the molecules that were studied. We also demonstrate that the pseudopotential calculations gave excellent results for the lanthanum, actinium and lawrencium compounds. However, the large frozen core in lutetium limits the flexibility of the 4f-electrons significantly. This only has an effect at the correlated level and shows that even if the Dirac–Hartree–Fock method may be useful for benchmarking, agreement between an approximate and a fully relativistic method at the SCF level does not prove that the same will be the case at the correlated level.

The calculations in Paper IV have been performed by the author of this thesis. The new four-index transformation has been implemented by the author of this thesis in cooperation with L. Visscher and T. Saue.

Chapter 5

Concluding remarks

The study of transition metal, lanthanide and actinide chemistry has been a growth area of quantum chemistry the last decade. For the heavier of these elements use of relativistic methods both efficiently and accurately in the theoretical models is essential. The most accurate treatment of relativistic effects that is feasible today is by the use of four-component calculations based directly on the Dirac equation. These methods are now firmly established, and earlier doubts about their validity have been shown to be unfounded.

This thesis deals with various aspects of molecular relativistic four-component calculations, building on the earlier development of a direct four-component Dirac–Hartree–Fock program, DIRAC [21, 43], by T. Saue. The work presented here continues the development of four-component methods at the University of Oslo. Correlated four-component methods have been integrated as a part of DIRAC in the form of direct Möller-Plesset perturbation theory to second order (MP2). The direct methods employed in the Dirac–Hartree–Fock and MP2 modules make the program extremely well suited for calculations on high-performance workstations. While a number of groups around the world have developed Dirac–Hartree–Fock codes, only very few correlated four-component methods are available. After the implementation of the relativistic MP2 method in the DIRAC program system it is now possible to perform correlated calculations in addition to the mean-field calculations for quite large systems employing more than 1200 scalar Cartesian basis functions. The cost of the MP2 calculation is only a fraction of the cost of the full Dirac–Hartree–Fock procedure. It has been argued that the main utility of four-component Dirac–Hartree–Fock calculations lies in the calibration of other more approximate methods. In this respect the MP2 module serves a very important role since it allows the benchmarking of the *combined* effects of relativity and correlation. Hence approximate methods may be tested at the correlated level, the level at which these methods are most useful.

The MP2 method accounts for a majority of the correlation energy in heavy element

systems. It is therefore possible to investigate the coupling between relativistic and correlation effects in a method where no serious approximation is involved in the treatment of relativity. For many molecules it is also possible to obtain qualitatively reasonable values for a number of properties. The ratio of the cost of the MP2 method and for example the CCSD method is much more to the advantage of the former in the relativistic case than in the nonrelativistic. The reason is that in four-component calculations it is usually the four-index transformation that is the most expensive step. This tranformation involves much less work for the MP2 method than for any other correlated method. In this work the MP2 method has been applied to a few chemical problems of which the most important are the lanthanide and actinide contractions. The significance of relativity for these chemical trends has been demonstrated.

The second topic of this thesis is the study of the molecular wavefunction in the neighbourhood of a heavy nucleus. This is one of the first studies of parameters where the relativistic effects are extremely important and for example much more important than correlation effects. The basis set requirements for these calculations have been established. It has furthermore been demonstrated that the full flexibility of the four-component methods is necessary in addition to uncontracted basis sets fulfilling the restricted kintetic balance condition. After a careful analysis and elimination of errors in a Dirac–Hartree–Fock study on thallium fluoride we have been able to place the most restrictive limits yet available on several fundamental physical quantities. These calculations, combined with results from low energy molecular beam experiments, provide important contributions to elementary particle physics.

This work is an important step in the development of more effective accurate quantum chemical methods without serious approximations in the treatment of relativistic effects. Sometimes a concern has been voiced that the potential of the four-component methods has not been fully utilized due to lack of manpower investment in the current codes, as compared to the nonrelativistic codes [120]. Our efforts are aimed at remedying this situation with the development of the relativistic MP2 program. It is hoped that it soon will become obvious also to researchers outside the field of four-component methods that the methods are competitive and extremely useful for calculations where it is advantageous to obtain results with only minor approximations in the treatment of relativistic effects. The author believes that in the near future the necessary manpower will indeeed be invested in this field, and the fully relativistic methods will obtain the popularity that they deserve.

Bibliography

[1] P.A.M. Dirac, Proc. R. Soc. A **123**, 714 (1929).

[2] *CRC handbook of chemistry and physics, 74th Ed.*, edited by D.R. Lide (CRC Press, Boca Raton, 1993), p. **9**-156, and later editions; P. Pyykkö, Z. Naturforsch. **47a**, 189 (1992).

[3] P.A.M. Dirac, Proc. R. Soc. A **117**, 610 (1928); P.A.M. Dirac, Proc. R. Soc. A **118**, 351 (1928).

[4] B. Swirles, Proc. R. Soc. A **152**, 625 (1935).

[5] Harry M. Quiney (personal communication). The information is provided in a letter from Lady Jeffreys (née B. Swirles) to H.M.Q., 3 March 1997.

[6] P. Pyykkö, Chem. Rev. **88**, 563 (1988).

[7] K. Balasubramanian, J. Phys. Chem. **93**, 6585 (1989).

[8] P. Pyykkö, Adv. Quant. Chem. **11**, 353 (1978).

[9] K.S. Pitzer, Acc. Chem. Res. **12**, 271 (1979).

[10] P. Pyykkö and J.P. Desclaux, Acc. Chem. Res. **12**, 276 (1979).

[11] P. Pyykkö, in *The effects of relativity in atoms, molecules and the solid state*, edited by S. Wilson, I.P. Grant, and B.L. Gyorffy (Plenum Press, New York, 1991).

[12] C.C.J. Roothaan, Rev. Mod. Phys. **23**, 69 (1951); C.C.J. Roothaan and P.S. Bagus, in *Methods in Computational Physics*, edited by B. Alder, S. Fernbach and M. Rotenberg, **2**, 47 (1964).

[13] A.D. McLean and Y.S. Lee, in *Current aspects of quantum chemistry*, edited by R. Carbó (Elsevier, Amsterdam, 1981), vol. 21, p. 219; Y.S. Lee and A.D. McLean, J. Chem. Phys. **76**, 735 (1982).

[14] L. Visscher, O. Visser, P.J.C. Aerts, H. Merenga and W.C. Nieuwpoort, Comput. Phys. Commun. **81**, 120 (1994).

[15] A. Mohanty and E. Clementi, Int. J. Quant. Chem. **39**, 487 (1991).

[16] K.G. Dyall, in *Relativistic and electron correlation effects in molecules and solids*, edited by G.L. Malli (Plenum Press, New York, 1994).

[17] O. Matsuoka, J. Chem. Phys. **97**, 2271 (1992).

[18] A.K. Mohanty and F.A. Parpia, Phys. Rev. A **54**, 2863 (1996); F.A. Parpia, J. Phys. B: At. Mol. Opt. Phys. **30**, 3983 (1997).

[19] L. Pisani and E. Clementi, J. Comput. Chem. **15**, 466 (1994).

[20] H.M. Quiney, H. Skaane and I.P. Grant, Adv. Quant. Chem. (accepted).

[21] T. Saue, K. Fægri jr., T. Helgaker and O. Gropen, Mol. Phys. **91**, 937 (1997).

[22] J.E. Almlöf, K. Fægri jr. and K. Korsell, J. Comput. Chem. **3**, 385 (1982).

[23] R.J. Gould, Am. J. Phys. **64**, 597 (1996).

[24] C.D. Anderson, Phys. Rev. **41**, 405 (1932).

[25] M.E. Rose, *Relativistic electron theory* (Wiley, New York, 1961).

[26] R.E. Moss, *Advanced molecular quantum mechanics* (Chapman and Hall, London, 1973).

[27] T.P. Das, *Relativistic quantum mechanics of electrons* (Harper & Row, New York, 1973).

[28] J.D. Bjorken and S.D. Drell, *Relativistic quantum mechanics* (McGraw-Hill, New York, 1964).

[29] H.A. Bethe and E.E. Salpeter, *Quantum mechanics of one- and two-electron atoms* (Plenum Press, New York, 1977).

[30] E.U. Condon and G.H. Shortley, *The theory of atomic spectra* (Cambridge University Press, Cambridge, 1935).

[31] W.H.E. Schwarz, E.M. van Wezenbeek, E.J. Baerends and J.G. Snijders, J. Phys. B: At. Mol. Opt. Phys. **22**, 1515 (1989).

[32] E.J. Baerends, W.H.E. Schwarz, P. Schwerdtfeger and J.G. Snijders, J. Phys. B: At. Mol. Opt. Phys. **23**, 3225 (1990).

[33] J.P. Desclaux, At. Data Nucl. Data Tables **12**, 311 (1973).

[34] T. Ziegler, J.G. Snijders and E.J. Baerends, Chem. Phys. Lett. **75**, 1 (1980).

[35] T. Ziegler, J.G. Snijders and E.J. Baerends, in *The challenge of d and f electrons*, edited by D.R. Salahub and M.C. Zerner (Am. Chem. Soc, 1989), p. 322.

[36] J.G. Snijders and P. Pyykkö, Chem. Phys. Lett. **75**, 5 (1980).

[37] I.P. Grant and H.M. Quiney, Adv. At. Mol. Phys. **23**, 37 (1988).

[38] Y. Ishikawa, R. Baretty and R.C. Binning jr., Chem. Phys. Lett. **121**, 130 (1985).

[39] Y. Ishikawa and H.M. Quiney, Int. J. Quantum Chem. Symp. **21**, 523 (1987).

[40] L. Visscher and K.G. Dyall, (http://theochem.chem.rug.nl/~luuk/FiniteNuclei) At. Data Nucl. Data Tables (accepted).

[41] O. Matsuoka, Chem. Phys. Lett. **140**, 362 (1987).

[42] O. Visser, P.J.C. Aerts, D. Hegarty and W.C. Nieuwpoort, Chem. Phys. Lett. **134**, 34 (1987).

[43] T. Saue, University of Oslo, Ph.D. thesis, 1996 (unpublished).

[44] K.G. Dyall, I.P. Grant, C.T. Johnson, F.A. Parpia, E.P. Plummer, Comput. Phys. Commun. **55**, 425 (1989).

[45] K.G. Dyall, P.R. Taylor, K. Fægri jr. and H. Partridge, J. Chem. Phys. **95**, 2583 (1991).

[46] The BERTHA [20] calculations were performed by H. Skaane.

[47] G. Breit, Phys. Rev. **34**, 553 (1929): G. Breit, Phys. Rev. **36**, 383 (1930).

[48] C.G. Darwin, Phil. Mag. **39**, 537 (1920).

[49] J.A. Gaunt, Proc. R. Soc. A **122**, 513 (1929).

[50] O. Gorceix, P. Indelicato and J.P. Desclaux, J. Phys. B: At. Mol. Opt. Phys. **20**, 639 (1987).

[51] I. Lindgren, J. Phys. B: At. Mol. Opt. Phys. **23**, 1085 (1990).

[52] E. Lindroth, A. Mårtensson-Pendrill, A. Ynnerman and P. Öster, J. Phys. B: At. Mol. Opt. Phys. **22**, 2447 (1989).

[53] H.M. Quiney, University of Oxford, D. Phil. thesis, 1987 (unpublished).

[54] J. Sucher, Phys. Rev. A **22**, 348 (1980); J. Sucher, Phys. Scripta **36**, 271 (1987).

[55] O. Visser, L. Visscher, P.J.C. Aerts and W.C. Nieuwpoort, Theor. Chim. Acta. **81**, 405 (1992).

[56] L. Visscher, T. Saue, W.C. Nieuwpoort, K. Fægri jr. and O. Gropen, J. Chem. Phys. **99**, 6704 (1993).

[57] L. Visscher and K.G. Dyall, J. Chem. Phys. **104**, 9040 (1996).

[58] L. Visscher, J. Styszyñski and W.C. Nieuwpoort, J. Chem. Phys. **105**, 1987 (1996).

[59] M. Born and R. Oppenheimer, Ann. Phys. (Leipzig) **84**, 457 (1927).

[60] M. Born and K. Huang, *Dynamical theory of crystal lattices* (Oxford University, London, 1954).

[61] P.M. Kozlowski and L. Adamowicz, Chem. Rev. **93**, 2007 (1993).

[62] H.H. Grelland, J. Phys. B: Atom. Molec. Phys. **13**, L389 (1980).

[63] A. Messiah, *Quantum mechanics* (North-Holland Publishing, Amsterdam, 1961).

[64] P. Hafner, J. Phys. B: Atom. Molec. Phys. **13**, 3297 (1980).

[65] I.P. Grant, Comput. Phys. Commun. **84**, 59 (1994).

[66] H.M. Quiney, H. Skaane, I.P. Grant and T.C. Scott, Proc. R. Soc. Lond. A (submitted).

[67] W.H. Furry, Phys. Rev. **81**, 115 (1951).

[68] J. Almlöf, in *Modern electronic structure theory, I*, edited by D.R. Yarkony (World Scientific, Singapore, 1995).

[69] P. Pulay, Chem. Phys. Lett. **73**, 393 (1980); P. Pulay, J. Comput. Chem. **3**, 556 (1982).

[70] DIIS was implemented in cooperation with T. Saue (See also [21]).

[71] P.O. Löwdin, Adv. Chem. Phys. **2**, 207 (1959).

[72] L. Visscher, University of Groningen, Ph.D. thesis, 1993 (unpublished).

[73] E. Eliav and U. Kaldor, Chem. Phys. Lett. **248**, 405 (1996).

[74] L. Visscher, K.G. Dyall and T.J. Lee, Int. J. Quantum Chem. Symp. **29**, 411 (1995).

[75] E. Eliav, U. Kaldor and Y. Ishikawa, Phys. Rev. A **49**, 1724 (1994); E. Eliav, U. Kaldor, P. Schwerdtfeger, B.A. Hess and Y. Ishikawa, Phys. Rev. Lett. **73**, 3203 (1994); E. Eliav, U. Kaldor, Y. Ishikawa, M. Seth and P. Pyykkö, Phys. Rev. A **53**, 3926 (1996).

[76] H.J. Aa. Jensen, K.G. Dyall, K. Fægri jr. and T. Saue, J. Chem. Phys. **104**, 4083 (1996).

[77] H.M. Quiney (private communication).

[78] C. Møller and M.S. Plesset, Phys. Rev. **46**, 618 (1934).

[79] K.G. Dyall, Chem. Phys. Lett. **224**, 189 (1994).

[80] J.A. Pople, J.S. Binkley and R. Seeger, Int. J. Quantum Chem. Symp. **10**, 1 (1976).

[81] P. Jørgensen and J. Simons, *Second quantization-based methods in quantum chemistry* (Academic Press, New York, 1981).

[82] J. Sapirstein, Phys. Scripta **36**, 801 (1987).

[83] H.M. Quiney, I.P. Grant and S. Wilson, in *Lecture notes in chemistry*: **52**, edited by U. Kaldor (Springer, 1989).

[84] L. Visscher, T. Saue and J.K. Laerdahl (Several disk and internal memory based, integral-driven, direct four-index transformation schemes have been implemented in DIRAC. The theory will be presented in a separate paper).

[85] S.F. Boys, Proc. Roy. Soc. A **200**, 542 (1950); S.F. Boys, G.B. Cook, C.M. Reeves and I. Shavitt, Nature, **178**, 1207 (1956).

[86] T.U. Helgaker and P.R. Taylor, in *Modern electronic structure theory, Part II*, edited by D.R. Yarkony (World Scientific, Singapore, 1995).

[87] T. Helgaker, P.R. Taylor, K. Ruud, O. Vahtras and H. Koch, HERMIT, a Molecular Integral Program.

[88] Dalton, an electronic structure program, Release 1.0 (1997), written by T. Helgaker, H. J. Aa. Jensen, P. Jørgensen, J. Olsen, K. Ruud, H. Ågren, T. Andersen, K. L. Bak, V. Bakken, O. Christiansen, P. Dahle, E. K. Dalskov, T. Enevoldsen, B. Fernandez, H. Heiberg, H. Hettema, D. Jonsson, S. Kirpekar, R. Kobayashi, H. Koch, K. V. Mikkelsen, P. Norman, M. J. Packer, T. Saue, P. R. Taylor, and O. Vahtras.

[89] The basis sets have been optimized by the author in cooperation with K. Fægri jr.

[90] M.W. Schmidt and K. Ruedenberg, J. Chem. Phys. **71**, 3951 (1979).

[91] H.M. Quiney (personal communication).

[92] Y.K. Kim, Phys. Rev. **154**, 17 (1967); Y.K. Kim, Phys. Rev. **159**, 190 (1967); F. Mark and F. Rosicky, Chem. Phys. Lett. **74**, 562 (1980); H. Wallmeier and W. Kutzelnigg, Chem. Phys. Lett. **78**, 341 (1981).

[93] W.H.E. Schwarz and H. Wallmeier, Mol. Phys. **46**, 1045 (1982).

[94] W. Kutzelnigg, Int. J. Quant. Chem. **25**, 107 (1984).

[95] Y. Ishikawa, R.C. Binning jr. and K.M. Sando, Chem. Phys. Lett. **101**, 111 (1983).

[96] R.E. Stanton and S. Havriliak, J. Chem. Phys. **81**, 1910 (1984).

[97] K.G. Dyall, I.P. Grant and S. Wilson, J. Phys. B: Atom. Molec. Phys. **17**, 493 (1984).

[98] H.M. Quiney, I.P. Grant and S. Wilson, Phys. Scripta **36**, 460 (1987).

[99] J.D. Talman, Phys. Rev. Lett. **57**, 1091 (1986); L. LaJohn and J.D. Talman, Chem. Phys. Lett. **189**, 383 (1992).

[100] G.E. Brown and D.G. Ravenhall, Proc. R. Soc. A **208**, 552 (1951).

[101] M.H. Mittleman, Phys. Rev. A **24**, 1167 (1981).

[102] R. McWeeny, *Methods of molecular quantum mechanics* (Academic press, London, 1992), 2nd ed., p. 38.

[103] W. Kutzelnigg, Phys. Scripta **36**, 416 (1987).

[104] K.G. Dyall, *Introduction to relativistic quantum chemistry*, a course for graduate students (lecture notes), Chemistry Dept., University of Odense, Denmark (1995).

[105] K.G. Dyall and K. Fægri jr., Chem. Phys. Lett. **174**, 25 (1990).

[106] K.G. Dyall, K. Fægri jr. and P.R. Taylor, in *The effects of relativity in atoms, molecules and the solid state*, edited by S. Wilson, I.P. Grant and B.L. Gyorffy (Plenum Press, New York, 1991).

[107] T. Saue, J.K. Laerdahl, L. Visscher and H.J.Aa. Jensen (manuscript).

[108] P.O. Löwdin, Adv. Quant. Chem. **5**, 185 (1970).

[109] K.G. Dyall and K. Fægri jr., Theor. Chim. Acta. **94**, 39 (1996).

[110] K. Fægri jr. and J. Almlöf, J. Comput. Chem. **7**, 396 (1989).

[111] E.A. Hinds and P.G.H. Sandars, Phys. Rev. A **21**, 471 (1980).

[112] P.V. Coveney and P.G.H. Sandars, J. Phys. B: At. Mol. Phys. **16**, 3727 (1983).

[113] H.F. Schaefer III, J.R. Thomas, Y. Yamaguchi, B.J. DeLeeuw and G. Vacek, in *Modern electronic structure theory, I*, edited by D.R. Yarkony (World Scientific, Singapore, 1995).

[114] P. Schwerdtfeger, M. Dolg, W.H.E. Schwarz, G.A. Bowmaker and P.D.W. Boyd, J. Chem. Phys. **91**, 1762 (1989).

[115] C.L. Collins, K.G. Dyall and H.F. Schaefer III, J. Chem. Phys. **102**, 2024 (1995).

[116] M. Head-Gordon, J.A. Pople and M.J. Frisch, Chem. Phys. Lett. **153**, 503 (1988).

[117] F. A. Cotton and G. Wilkinson, *Advanced Inorganic Chemistry* (Wiley, New York, 1988), p. 956.

[118] W. Küchle, M. Dolg, and H. Stoll, *J. Phys. Chem.* (in press).

[119] K.G. Dyall, J. Chem. Phys. **98**, 9678 (1993).

[120] L. Visscher (private communication); H.M. Quiney (private communication).